nature immunology

ARTICLES

https://doi.org/10.1038/s41590-018-0085-3

# Resistance of HIV-infected macrophages to CD8+ T lymphocyte–mediated killing drives activation of the immune system

Kiera L. Clayton[1], David R. Collins[1,2], Josh Lengieza[1], Musie Ghebremichael[1], Farokh Dotiwala[3,4], Judy Lieberman[3,4] and Bruce D. Walker[1,2,5*]

**CD4+ T lymphocytes are the principal target of human immunodeficiency virus (HIV), but infected macrophages also contribute to viral pathogenesis. The killing of infected cells by CD8+ cytotoxic T lymphocytes (CTLs) leads to control of viral replication. Here we found that the killing of macrophages by CTLs was impaired relative to the killing of CD4+ T cells by CTLs, and this resulted in inefficient suppression of HIV. The killing of macrophages depended on caspase-3 and granzyme B, whereas the rapid killing of CD4+ T cells was caspase independent and did not require granzyme B. Moreover, the impaired killing of macrophages was associated with prolonged effector cell–target cell contact time and higher expression of interferon-γ by CTLs, which induced macrophage production of pro-inflammatory chemokines that recruited monocytes and T cells. Similar results were obtained when macrophages presented other viral antigens, suggestive of a general mechanism for macrophage persistence as antigen-presenting cells that enhance inflammation and adaptive immunity. Inefficient killing of macrophages by CTLs might contribute to chronic inflammation, a hallmark of chronic disease caused by HIV.**

Accumulating evidence suggests that infected macrophages contribute to the persistence and pathogenesis of human immunodeficiency virus (HIV). Whereas HIV-infected CD4+ T cells die within a few days of infection, in vitro studies suggest that macrophages are resistant to the cytopathic effects of HIV replication, which results in continuous viral propagation[1]. Moreover, infected macrophages efficiently disseminate virus to CD4+ T cells via neutralization-evading cell-to-cell spread[2–4]. Studies of animal models of HIV infection further support the proposal of in vivo infection and persistence of macrophages[5–8], even during combination antiretroviral therapy[6,8], and suggest that macrophages contribute to the pathogenesis of HIV[9]. In addition, infected myeloid cells and macrophages have been observed in the lungs, gut and lymph tissues of HIV-infected patients[10], as well as in the brain, which contributes to the development of HIV-associated neurocognitive disorder and dementia[11]. Finally, macrophage-associated diseases, such as atherosclerosis, metabolic diseases and cancer, have been described in HIV+ subjects[12], with chronic inflammation contributing to these comorbidities, which afflict patients treated with combination antiretroviral therapy[13].

CD8+ cytotoxic T lymphocytes (CTLs) control viral levels during acute and chronic stages of HIV infection and reduce the progression of disease caused by HIV[14,15]. Most studies have focused on the control of infected CD4+ T cells by CTLs, with less focus on infected macrophages. Published work has shown that HIV-specific CTLs can eliminate HIV-infected macrophages in vitro[16–19]. However, the efficiency of CTL-mediated killing of HIV-infected CD4+ T cells relative to that of HIV-infected macrophages is poorly characterized. Studies suggest that macrophages infected with simian immunodeficiency virus (SIV) are relatively resistant to being killed by CTLs, but the mechanism behind their differential susceptibility is unknown[20,21]. In fact, the killing of infected macrophages by CTLs, unlike that of CD4+ T cells, appears to be relatively unaffected by downregulation of major histocompatibility complex (MHC) class I mediated by the immunosuppressive HIV protein Nef[16,20]. Improved understanding of CTL responses to HIV-infected macrophages will inform strategies to eliminate this population and combat HIV-associated inflammation.

Here we characterized and compared the interactions of HIV-specific ex vivo CTLs with HIV-infected CD4+ T cell targets and macrophage targets. We found that macrophages were less susceptible to CTL-mediated killing than were CD4+ T cells and that this was an intrinsic characteristic of macrophages independent of HIV infection. Although CTL cytotoxic granules mediated the killing of both cell types, CD4+ T cells underwent rapid caspase-independent cell death, while macrophages underwent a slower granzyme B– and caspase-3-dependent death. Inefficient CTL-mediated killing of macrophages drove prolonged formation of synapses between effector cells and target cells, greater secretion of IFN-γ (a major macrophage-activating cytokine) from CTLs and induction of macrophage pro-inflammatory chemokines that recruited monocytes and T cells. Furthermore, we obtained similar results for responses to cytomegalovirus (CMV), Epstein-Barr virus (EBV) and influenza virus (Flu), which indicates that delayed killing of macrophages by CTLs might be a general mechanism whereby antigen-presenting cells promote inflammation.

## Results

**HIV-infected macrophages are inefficiently killed by CTLs.** We developed an in vitro system to simultaneously study the interactions of freshly isolated ('ex vivo') CTLs with HIV-infected CD4+ T cells and macrophages (Supplementary Fig. 1). Because patients

[1]Ragon Institute of MGH, MIT and Harvard, Cambridge, MA, USA. [2]Howard Hughes Medical Institute, Chevy Chase, MD, USA. [3]Program in Cellular and Molecular Medicine, Boston Children's Hospital, Boston, MA, USA. [4]Department of Pediatrics, Harvard Medical School, Boston, MA, USA. [5]Institute of Medical Engineering and Sciences, Massachusetts Institute of Technology, Cambridge, MA, USA. *e-mail: bwalker@mgh.harvard.edu

who control HIV by spontaneously keeping plasma viremia below 50 RNA copies per ml ('elite controllers') or between 50 and 2,000 RNA copies per ml ('viremic controllers') exhibit potent ex vivo CTL responses to infected CD4+ T cells[22] and macrophages[18,19], we used samples from such patients for this study. Monocyte-derived macrophages (differentiated through the use of the growth factors GM-CSF and M-CSF) and activated CD4+ T cells were infected with HIV and co-cultured with autologous ex vivo CTLs (isolated through the use of negative enrichment kits that deplete samples of natural killer cells). The elimination of HIV-infected target cells positive for the group-specific antigen capsid protein Gag p24 was assessed by flow cytometry after 4 h of co-culture (Fig. 1a,b and Supplementary Fig. 2). Infected CD4+ T cells were more efficiently eliminated by autologous ex vivo CTLs (57.0% ± 5.5% (mean ± s.e.m.) residual Gag+ targets at an effector cell/target cell ratio of 4:1) than were infected macrophages (94.3% ± 1.8% residual Gag+ targets). Killing was HIV specific, as indicated by the lack of killing by ex vivo CTLs from uninfected healthy donors (Fig. 1b). Similar results were obtained with monocyte-derived macrophages differentiated through the use of human serum ($P < 0.0001$ (two-sided unpaired $t$-test); Supplementary Fig. 3a), which suggested that this resistance to CTL-mediated killing was a general feature of macrophages, not solely of macrophages derived with GM-CSF, M-CSF or fetal bovine serum. To further evaluate the susceptibility of macrophages to CTL-mediated killing, we employed CTL effector populations that had been expanded via HIV peptide, which have been shown to kill macrophages within 4–24 h (refs.[16,18,20]). These 'peptide-expanded CTLs' killed HIV-infected macrophages within 4 h of co-culture (65.0% ± 7.8% residual Gag+ targets; Fig. 1c). However, infected macrophages still survived significantly more than did infected CD4+ T cells (39.8% ± 5.3% residual Gag+ targets). Together these data indicated that HIV-infected macrophages were more resistant to CTL-mediated killing than were infected CD4+ T cells.

**Resistance to CTL-mediated killing is an intrinsic characteristic of macrophages.** HIV infection enhances the survival of macrophages through multiple proposed mechanisms[1] that might mediate resistance to being killed by CTLs. To determine whether infection-associated differences in the survival of macrophages might explain the differences between infected CD4+ T lymphocyte targets and their macrophage counterparts in the context of killing or whether this was an intrinsic property of macrophages, we next performed killing assays using uninfected, peptide-loaded macrophages and activated CD4+ T cells (Fig. 1d,e). HIV peptide–loaded macrophages were significantly more resistant to killing mediated by expanded CTLs (72.0% ± 3.0% (mean ± s.e.m.) residual peptide-loaded targets) than were CD4+ T lymphocytes (8.4% ± 1.8% residual peptide-loaded targets). Similar results were obtained with ex vivo CTLs (Supplementary Fig. 3b). Furthermore, there was no difference between the killing of activated CD4+ T cells by CTLs and that of resting ex vivo CD4+ T cells (Supplementary Fig. 3c), which suggested that the enhanced sensitivity of CD4+ T cells to CTL-mediated killing was not an effect of activation. To determine whether these results could be extended beyond HIV, we loaded target cells simultaneously with peptides from CMV, EBV and Flu (CEF peptides) and cultured those cells with CEF peptide–expanded CTLs from HIV- donors. Similar to HIV peptide–loaded cells, CEF peptide–loaded macrophages exhibited greater resistance to CTL-mediated killing (65.6% ± 10.7% residual peptide-loaded targets) than did their CD4+ T cell counterparts (14.6% ± 3.4% residual peptide-loaded targets) (Fig. 1f). Together these results indicated that resistance to CTL-mediated killing was an intrinsic feature of macrophages that did not depend on the mode of cell differentiation or HIV infection.

**Macrophages, unlike CD4+ T cells, die by slow caspase-3-dependent apoptosis, which results in inefficient viral suppression.** The elimination assay used above measured the effect of HIV-specific CTLs on the survival of infected cells following a short incubation. To determine whether macrophages might still be killed, but more slowly, we co-cultured ex vivo CTLs with peptide-loaded CD4+ T cells or macrophages for up to 24 h and monitored target-cell survival over time. In contrast to the killing of peptide-loaded CD4+ T cells, which was detected within 4 h, the killing of macrophages was delayed until 12 h (Fig. 2a). Furthermore, at the 24-hour time point, significantly more CD4+ T cells (50.0% ± 5.5% (mean ± s.e.m.) residual peptide-loaded targets) than macrophages (72.3% ± 2.0% residual peptide-loaded targets) were eliminated. Similar trends were observed with expanded CTL effectors (Supplementary Fig. 4). Thus, for the macrophages that succumbed to CTL-mediated killing, the kinetics of cell death were slower than those of activated CD4+ T cells.

We next assessed the ability of CTLs to mediate viral suppression in macrophages and CD4+ T cells. We monitored Gag p24 in the supernatants of HIV-infected CD4+ T cells or macrophages cultured for 7 d with or without ex vivo CTLs (Fig. 2b). The infection of CD4+ T cells was robustly suppressed on day 3 of co-culture (82.3% ± 2.0% (mean ± s.e.m.) reduction in p24 compared with that of cultures without CTLs) and plateaued on day 5 of co-culture (92.6% ± 1.1% reduction in p24). In contrast, ex vivo CTLs were less efficient at suppressing macrophage infection after 3 d of co-culture (53.1% ± 6.2% reduced p24). The inhibition of macrophage infection remained significantly less than the inhibition of CD4+ T cell infection, even after 7 d of culture. These data indicated that the slow killing of macrophages resulted in less-efficient suppression of HIV infection in macrophages than in CD4+ T cells.

On the basis of those results, we hypothesized that different mechanisms of cell death might explain the relative delay in the killing of macrophages. CTLs trigger both caspase-dependent cell-death pathways and caspase-independent cell-death pathways. We assessed activation of caspase-3 (the main 'executioner' caspase[23]) in live HIV-infected target cells after 4 h of co-culture with effector cells (Fig. 2c,d). HIV-infected macrophages exhibited significantly more caspase-3 activity than that of infected CD4+ T cell targets following co-culture with expanded CTLs, as measured by an indicator of caspase-3 activity. In contrast, live CD4+ T cells exhibited significantly increased levels of reactive oxygen species (ROS) (that result from disruption of the mitochondria, which occurs in both caspase-dependent killer cell–mediated programmed cell death and its caspase-independent counterpart[24]) following co-culture with CTLs (Fig. 2e,f). Furthermore, co-culture of expanded CTLs with peptide-loaded target cells treated with either a pan-caspase inhibitor or an inhibitor of caspase-3 did not inhibit the killing of CD4+ T cells but dramatically blocked the killing of macrophages (the frequency of residual peptide-loaded targets increased from 65.7% ± 5.3% (mean ± s.e.m.) in the control condition to 105.1% ± 2.0% with the pan-caspase inhibitor and 100.5% ± 3.9% with the inhibitor of caspase-3; Fig. 2g). As a control, necrostatin-1, which blocks necroptosis (an alternative programmed cell-death pathway[25]), did not inhibit the killing of target cells. These data suggested that the macrophages died by caspase-3-dependent apoptosis, whereas the CD4+ T cells died by a caspase-independent process.

**CTL killing of macrophages, but not that of CD4+ T cells, requires granzyme B.** We next sought to further investigate the mechanism by which CTLs initiate caspase-3-dependent macrophage death. CTLs kill their target cells either by releasing their cytotoxic granules or by engaging death receptors, such as FAS or TRAIL, which trigger caspase-mediated apoptosis[26]. Granule-mediated killing can be either caspase independent or caspase dependent, depending on which granzymes are involved and whether the target cell is

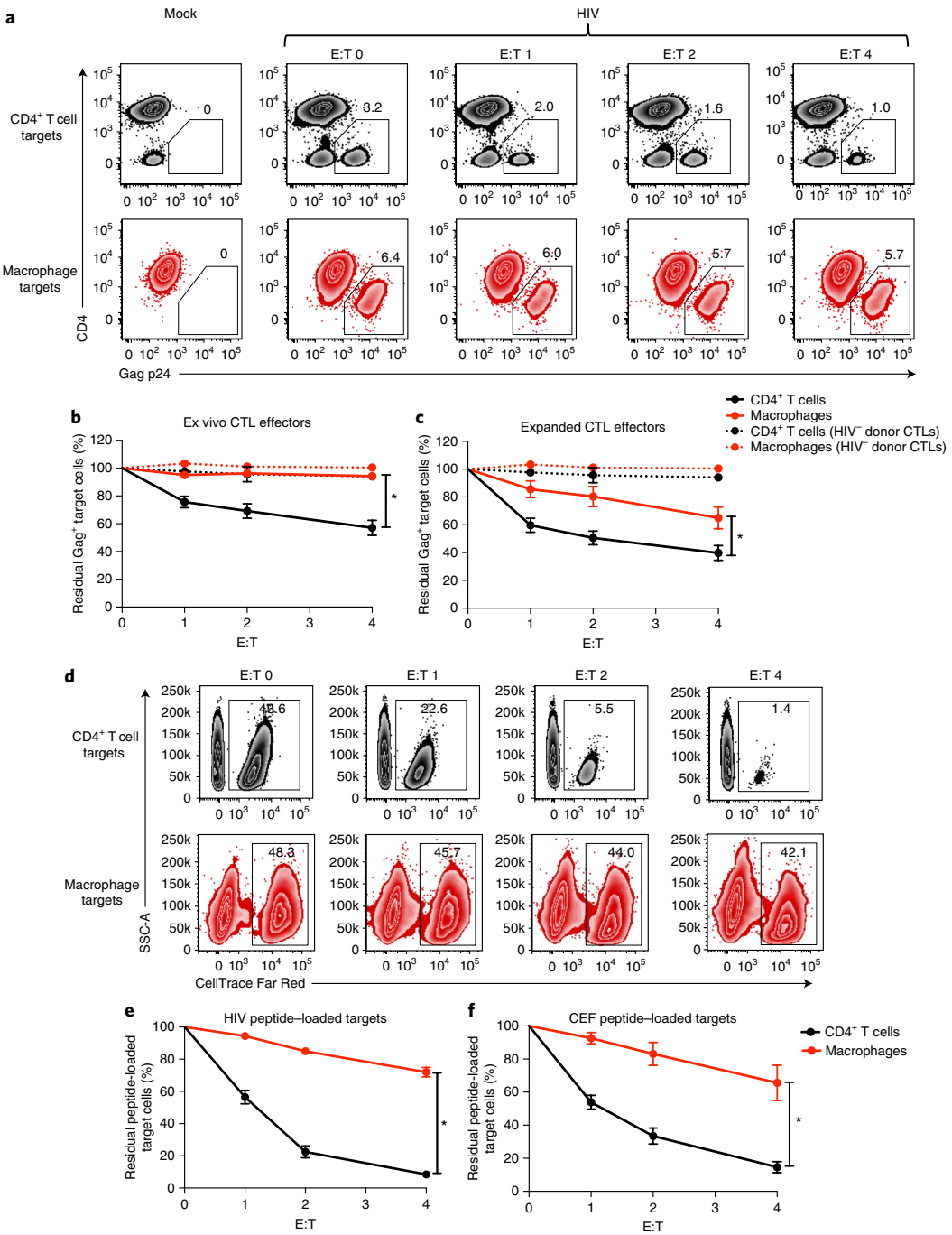


**Fig. 1 | HIV-infected macrophages are less susceptible to CTL-mediated killing than are HIV-infected CD4⁺ T cells. a**, Flow cytometry of cells from cultures of mock-infected (far left) or HIV-infected (middle and right) CD4⁺ T cells (top row) or macrophages (bottom row) co-cultured for 4 h, at various effector cell/target cell ratios (E:T) (above plots), with CTL effectors (additional information, Supplementary Figs. 1 and 2). Numbers adjacent to outlined areas indicate percent live infected cells with low to negative surface staining of CD4 and positive intracellular staining of Gag p24. Data are from one experiment representative of four independent experiments. **b**,**c**, Elimination assay of CD4⁺ T cells or macrophages (key) cultured at various effector cell/target cell ratios (E:T) (horizontal axis) with ex vivo CTLs (**b**) or HIV peptide–expanded CTLs (**c**) from HIV-infected donors, or CTLs from healthy HIV⁻ donors, as a negative control (key). *$P < 0.0001$ (**b**) or 0.0121 (**c**) (two-sided unpaired *t*-test). Data are from four independent experiments with $n = 16$ individual samples (HIV-infected donors) or two independent experiments with $n = 3$ individual samples (HIV⁻ donors) (mean ± s.e.m.). **d**, Flow cytometry of cells from co-cultures of activated CD4⁺ T cells or macrophages (left margin), with 50% of each target-cell population loaded with HIV peptides and stained with the proliferation dye CellTrace Far Red, cultured for 4 h, at various ratios (above plots), with autologous HIV peptide–expanded CTLs from an HIV⁺ donor. Numbers in outlined areas indicate percent Far Red⁺ peptide-loaded target cells. Data are from one experiment representative of two independent experiments. **e**, Elimination assay of HIV peptide–loaded CD4⁺ T cell or macrophage targets (key) cultured at various ratios (horizontal axis) with CTLs from HIV⁺ donors (additional information, Supplementary Fig. 3). *$P < 0.0001$ (two-sided unpaired *t*-test). Data are from two independent experiments with $n = 8$ individual samples (mean ± s.e.m.). **f**, Elimination assay of CEF peptide–loaded CD4⁺ T cell or macrophage targets (key) cultured at various ratios (horizontal axis) with CEF-specific CTLs from HIV⁻ donors. *$P = 0.0011$ (two-sided unpaired *t*-test). Data are from three independent experiments with $n = 6$ individual samples (mean ± s.e.m.).

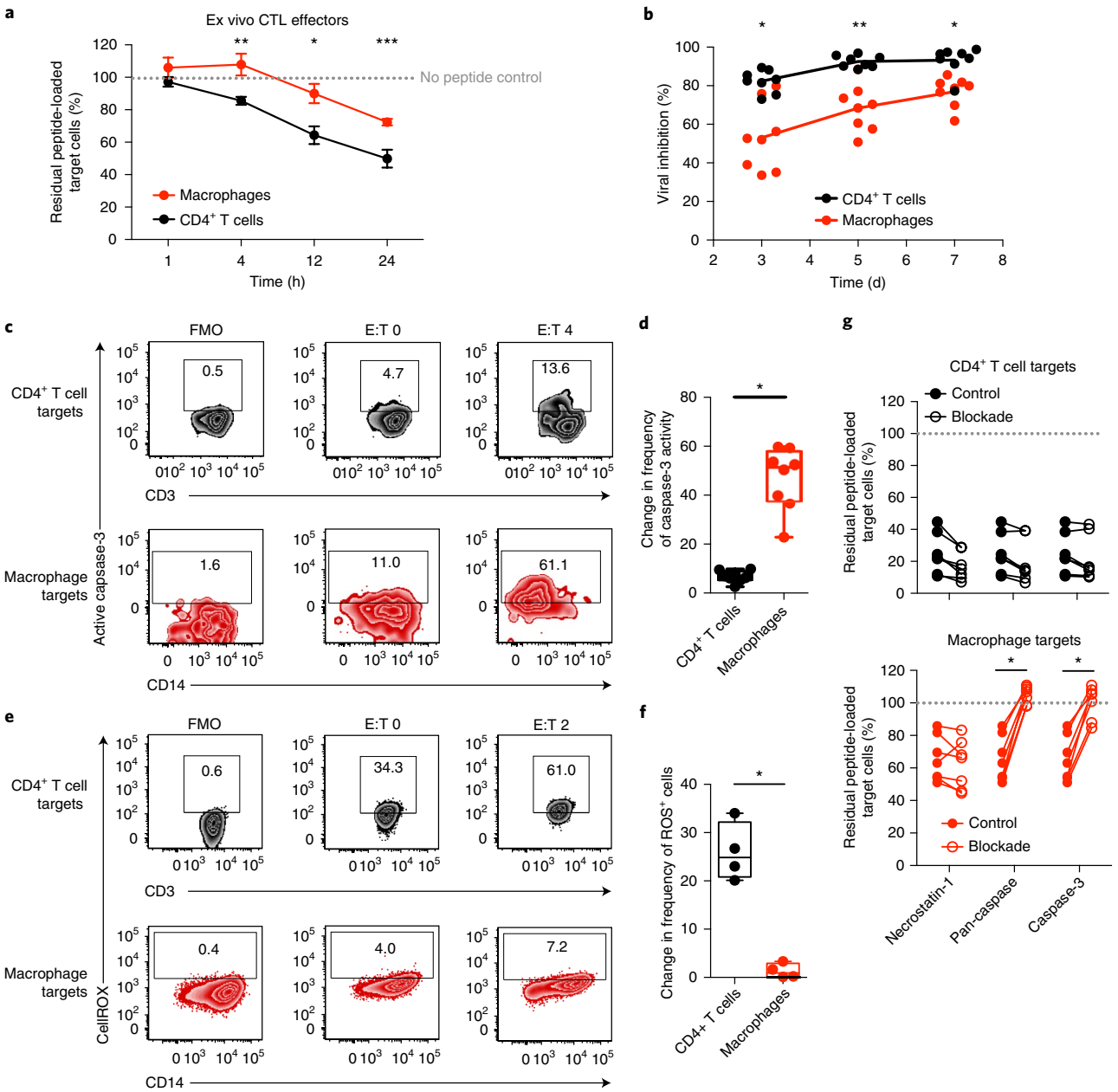


**Fig. 2 | CTLs induce delayed, caspase-3-dependent apoptosis of macrophages, which results in less-efficient control of HIV infection. a**, Time course for the killing of peptide-loaded target cells (key) incubated for various times (horizontal axis) with ex vivo CTLs from HIV$^+$ donors, analyzed by flow cytometry for the staining of live cells with CellTrace Far Red (additional information, Supplementary Fig. 4); dotted lined indicates control condition of cells not loaded with peptide, set as 100%. *$P = 0.0201$, **$P = 0.0165$ and ***$P = 0.0156$ (two-sided unpaired *t*-test). Data are from two independent experiments with $n = 4$ individual samples (mean ± s.e.m.). **b**, Virus-inhibition assay of ex vivo CTLs from HIV$^+$ donors cultured for 7 d with HIV-infected CD4$^+$ T cells or macrophages (key), assessed by measurement of Gag p24 in culture supernatants. *$P = 0.0005$ and **$P < 0.0001$ (two-sided unpaired *t*-test). Data are from three independent experiments with $n = 8$ individual samples per group (one per symbol at each time point). **c**, Flow cytometry of live peptide-loaded target cells (left margin) incubated at various ratios (above plots) with ex vivo CTLs from HIV$^+$ donors (as in Fig. 1a), assessing caspase-3 activity. FMO, fluorescence minus one (staining control). Numbers in outlined areas indicate percent live CD4$^+$ T cells (top row) or macrophages (bottom row) with active caspase-3. Data are from one experiment representative of two independent experiments. **d**, Caspase-3 activity in live target cells (horizontal axis) cultured with expanded CTLs from HIV$^+$ donors, presented as the absolute change in caspase-3 activity. Data are from two independent experiments with $n = 8$ individual samples (one per symbol) (box elements: center line, median; box top and bottom, 25th and 75th percentile; whiskers, minimum and maximum). $P < 0.0001$ (two-sided unpaired *t*-test). **e**, Flow cytometry of live target cells (left margin) cultured at various ratios (above plots) with expanded CTLs from HIV$^+$ donors (as in Fig. 1d), assessing ROS via the oxidative-stress indicator CellROX. Numbers in outlined areas indicate percent CellROX$^+$ live CD4$^+$ T cells (top row) or macrophages (bottom row). Data are from one experiment with one sample representative of four samples. **f**, Absolute change in the frequency of ROS$^+$ live target cells (horizontal axis) cultured with expanded CTLs from HIV$^+$ donors, assessing oxidative stress in live cells. *$P = 0.0002$ (two-sided unpaired *t*-test). Data are from one experiment with $n = 4$ individual samples (one per symbol; boxes as in **d**). **g**, Elimination assay of peptide-loaded CD4$^+$ T cells (top) or macrophages (bottom) as targets, pre-treated with various inhibitors (horizontal axis; Blockade) or not (Control) (key) and then cultured for 4 h with expanded CTLs from HIV$^+$ donors (analyzed as in **a**). *$P < 0.0001$ (two-sided paired *t*-test). Data are from two independent experiments with $n = 7$ individual samples (one per symbol; lines connect samples from the same donor).

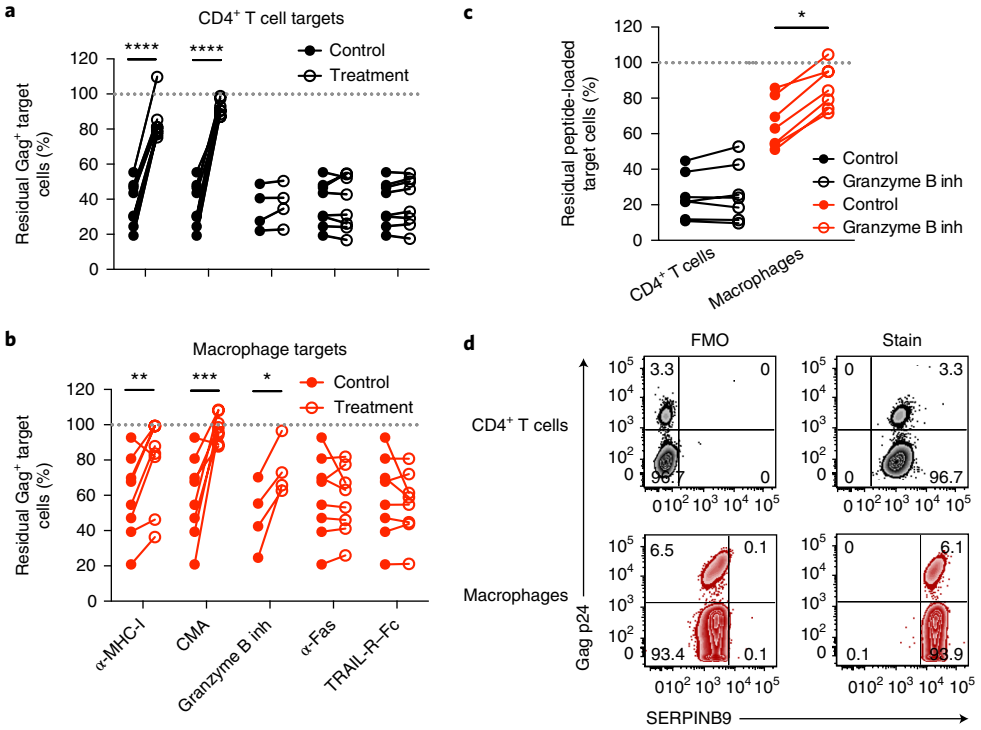


**Fig. 3 | Killing of target cells is dependent on MHC class I and perforin, but granzyme B is dispensable for the killing of CD4+ T cells. a**,**b**, Elimination assay of HIV-infected CD4+ T cells (**a**) or macrophages (**b**) after incubation for 4 h with HIV peptide–expanded CTLs from HIV+ donors in the presence (Treatment) or absence (Control) (key) of an MHC class I–blocking antibody (α-MHC-I), an indirect inhibitor of perforin (CMA), an inhibitor of granzyme B (Granzyme B inh), a FAS-neutralizing antibody (α-FAS) or recombinant human TRAIL-R1–Fc (horizontal axis), analyzed by flow cytometry for the intracellular staining of Gag p24 in live target cells. *$P = 0.0153$, **$P = 0.0097$, *** $P = 0.0036$ and ****$P < 0.0001$ (two-sided paired *t*-test). Data are from four independent experiments with $n = 8$ individual samples (lines connect samples from the same donor). **c**, Elimination of peptide-loaded, activated CD4+ T cells or macrophages (horizontal axis) by HIV peptide–expanded CTLs obtained from HIV+ donors and pre-incubated for 1 h with an inhibitor of granzyme B or not (key) before co-culture. *$P < 0.0001$ (two-sided unpaired *t*-test). Data are from two independent experiments with $n = 7$ individual samples (lines connect samples from the same donor). **d**, Flow-cytometry analysis of the intracellular staining of Gag p24 and the granzyme B inhibitor SERPINB9 in HIV-infected CD4+ T cell and macrophages (left margin). Numbers in quadrants indicate percent cells in each. Data are from one experiment representative from three independent experiments.

resistant to caspase-mediated cell death[27]. To determine the mechanism of CTL-mediated killing, we cultured HIV-infected target cells and effector cells together in the presence of an MHC class I–blocking antibody to prevent engagement of the T cell antigen receptor; concanamycin A (CMA) to indirectly inhibit perforin[28]; a granzyme B–specific inhibitor (Ac-IETD-CHO); a FAS-neutralizing antibody; or recombinant TRAIL-R1–Fc protein to block engagement of TRAIL (Fig. 3a,b). The killing of both HIV-infected CD4+ T cells and HIV-infected macrophages was blocked by the MHC class I–blocking antibody and by CMA, whereas blockade of FAS or TRAIL had no effect, which suggested that the killing of target cells by CTLs was mediated by recognition of MHC class I–restricted T cell antigen receptors that triggered granule exocytosis and granule-mediated death. Specific blockade of granzyme B inhibited the killing of HIV-infected or peptide-loaded macrophages (Fig. 3b,c) but had no effect on the killing of their CD4+ T cell counterparts (Fig. 3a,c). Together with the observations from Fig. 2, these data suggested that the killing of macrophages by CTLs was mediated by granzyme B and subsequent activation of caspase-3 (Fig. 2c,d,g), while the killing of CD4+ T cells might have been mediated by alternative granzymes (other than granzyme B) that disrupted the mitochondria (as indicated by the increase in ROS) to induce caspase-independent programmed cell death (Fig. 2e–g). Both CD4+ T cells and macrophages had high expression of SERPINB9, a natural inhibitor of granzyme B[27] (Fig. 3d), which suggested that both target cells might be resistant to granzyme B. Given that the killing of macrophages by CTLs requires granzyme B, expression of SERPINB9 probably delayed the initiation of granzyme B–mediated cell death (similar to overexpression of the pro-survival factor Bcl-2[29]), which could explain the slower timing of macrophage apoptosis relative to that of CD4+ T cells.

**HIV-specific CTLs exhibit low co-expression of perforin and granzyme B.** The ex vivo CTL–mediated killing of HIV-infected macrophages was significantly lower than such killing of HIV-infected CD4+ T cells (Figs. 1b and 2a). However, the killing of macrophages improved when expanded CTLs were engaged as effector cells (Fig. 1c and Supplementary Fig. 4). To assess the cytolytic potential of both effector-cell populations, we first stained ex vivo CTLs with a pool of HIV tetramers matched to each subject's HLA molecules and then assessed their expression of perforin and granzyme, with staining of naive T cells serving as a negative control (Supplementary Fig. 5a). Although the majority of HIV-specific cells expressed granzymes (frequency (mean values) of cells with expression of granzyme A, ~26%; granzyme B, 60%; granzyme H, 54%; granzyme K, 67%; and granzyme M, 79%), the frequency of cells co-expressing perforin and granzyme (representative of the cytolytic population) was lower (co-expression of perforin with granzyme A, ~9%; with granzyme B, 21%; with granzyme H, 20%; with granzyme K, 7%; and with granzyme M, 30%) (Fig. 4a–c). This was not an effect of poor ex vivo staining of CTLs, as CMV-specific ex vivo CTLs exhibited high co-expression of perforin and

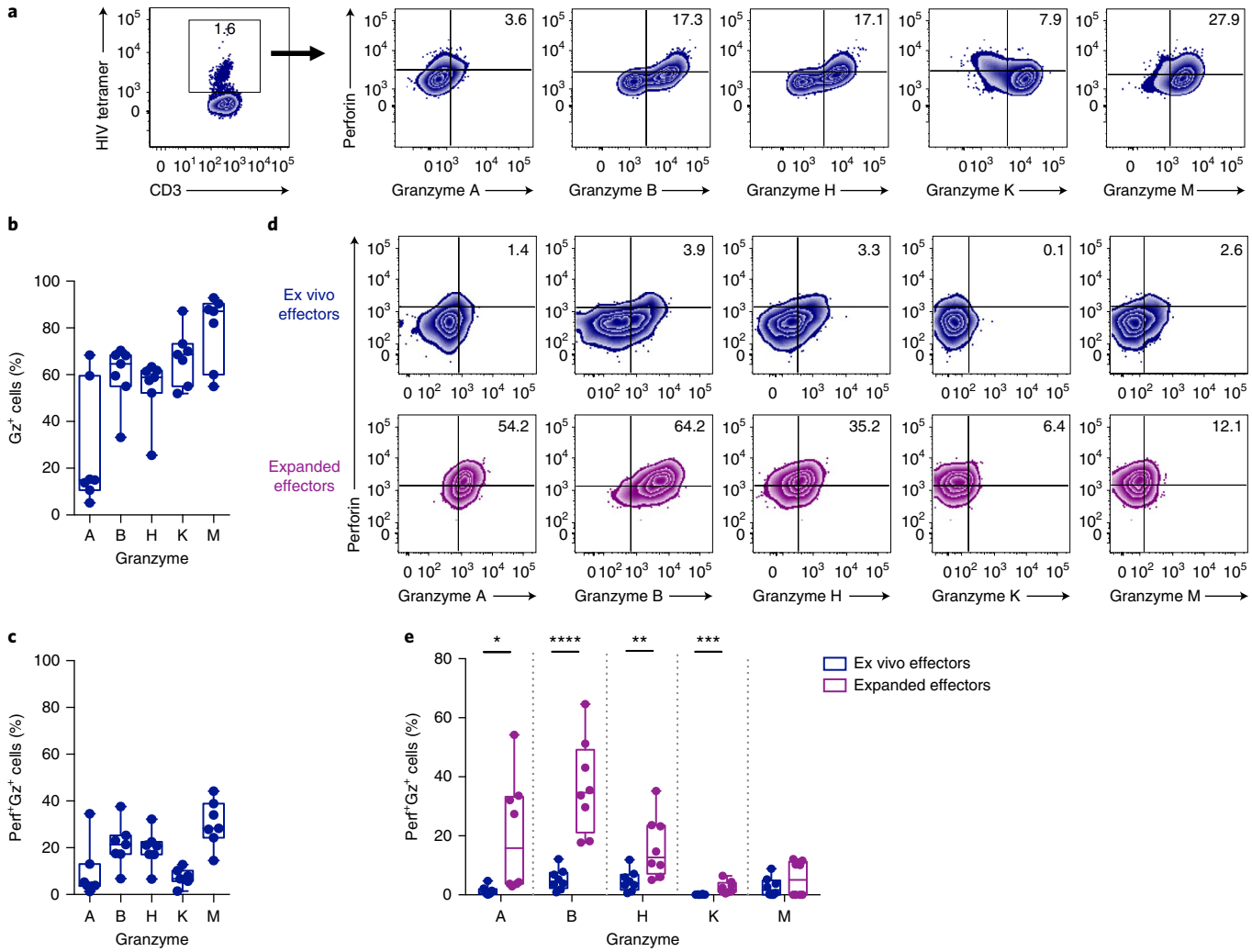


**Fig. 4 | Ex vivo HIV-specific CTLs exhibit lower expression of perforin and granzymes than that of expanded CTLs. a**, Flow cytometry of ex vivo HIV tetramer–positive CD8⁺ T cells (gated as at far left; A02-SL9 (HIV) tetramer), assessing the staining of perforin and granzyme A, B, H, K or M (middle and right) (staining controls, Supplementary Fig. 5a,b; CMV-specific CTL expression of perforin and granzyme, Supplementary Fig. 5c). Numbers in quadrants indicate percent cells in each. Data are from one experiment representative of two independent experiments. **b**, Total expression of various granzymes (horizontal axis) on HIV-specific ex vivo CTLs from HIV⁺ controllers, presented as the frequency of granzyme-positive (Gz⁺) cells. Data are from two independent experiments with $n = 7$ individual samples (one per symbol; boxes as in Fig. 2d). **c**, Dual expression of perforin and various granzymes (horizontal axis) on HIV-specific ex vivo CD8⁺ T cells, presented as the frequency of perforin-positive, granzyme-positive (Perf⁺Gz⁺) cells. Data are from two independent experiments with $n = 7$ individual samples (one per symbol; boxes as in Fig. 2d). **d**, Flow cytometry of ex vivo or expanded CTLs (left margin) incubated for 6 h with HIV-infected CD4⁺ T cells, assessing the staining of perforin and granzyme A, B, H, K or M by degranulated cells (positive for surface expression of CD107a) (staining controls, Supplementary Fig. 5d). Numbers in quadrants indicate percent cells in each. Data are from one experiment representative of two independent experiments. **e**, Co-expression of perforin and various granzymes (horizontal axis) by degranulated ex vivo and expanded CTLs from HIV⁺ donors (presented as in **c**). $^{*}P = 0.0156$, $^{**}P = 0.0115$, $^{***}P = 0.005$, $^{****}P < 0.0001$ (two-tailed unpaired *t*-test). Data are from two independent experiments with $n = 8$ individual samples (one per symbol; boxes as in Fig. 2d).

granzymes (Supplementary Fig. 5c). Similar results were obtained by phenotyping of ex vivo CTLs that degranulated in response to HIV-infected target cells (CD107a⁺ cells; Fig. 4d,e; staining controls, Supplementary Fig. 5d). However, in vitro–expanded HIV-specific CTL effector populations exhibited a significantly greater frequency of cells positive for both perforin and granzymes (except granzyme M) than that of ex vivo CTL populations (Fig. 4d,e), in support of the proposal of enhanced cytolytic function of expanded CTLs relative to that of ex vivo CTLs. Comparison of the co-expression of perforin and granzymes in response to CD4⁺ T cells and macrophages revealed no differences between these (Supplementary Fig. 5e), which suggested that CTLs engaged by either target cell exhibited similar cytolytic potential.

**CTLs efficiently recognize HIV-infected macrophages and produce more IFN-γ in response to these cells.** Variations in the surface density of MHC class I could alter the recognition of target cells by CTLs and contribute to differences in elimination. To determine the density of MHC class I on the surface of CD4⁺ T cells relative to that of macrophages, we analyzed cells by imaging flow cytometry to calculate the surface area and mean fluorescence intensity of MHC class I (Supplementary Fig. 6a,b). There was no difference in the density of MHC class I on the surface of CD4⁺ T cells relative to that of macrophages (Fig. 5a), which suggested that the amount of antigen presented on macrophages, which have much greater surface area than that of T cells, could not explain the difference in killing. To investigate whether HIV-infected CD4⁺ T cells and

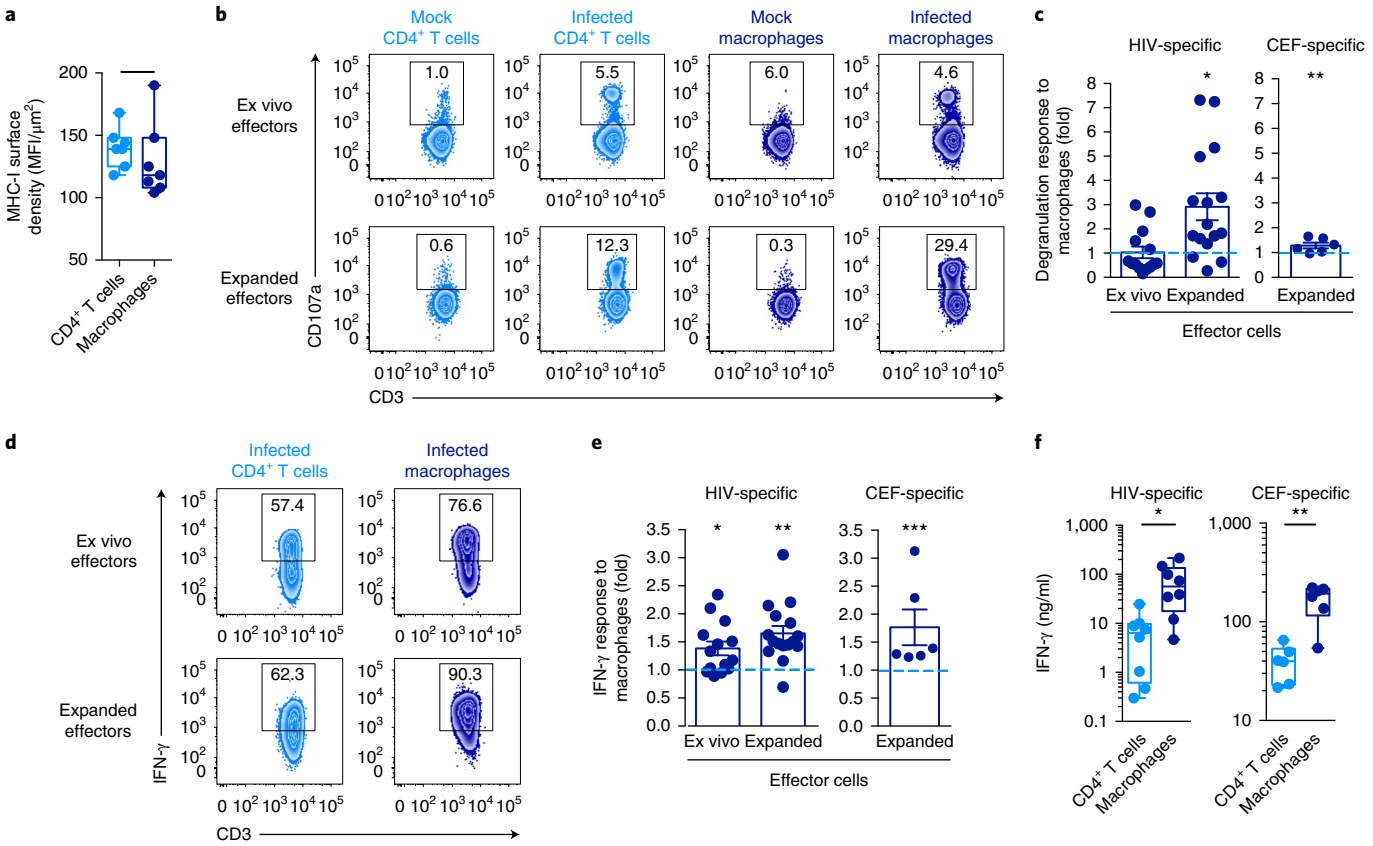


**Fig. 5 | HIV-infected macrophages induce stronger CTL cytokine responses than do infected CD4⁺ T cells. a**, Imaging flow cytometry assessing the surface density of MHC class I on CD4⁺ T cells and macrophages (horizontal axis) (additional information, Supplementary Fig. 6a,b). $P = 0.2209$ (two-sided Mann-Whitney test). Data are from three independent experiments with $n = 7$ individual samples (one per symbol; boxes as in Fig. 2d). **b**, Flow cytometry of ex vivo or expanded CTL effectors (left margin) incubated for 6 h with mock-infected (uninfected) or HIV-infected CD4⁺ T cells or macrophages (above plots), assessing degranulation (as CD107a expression) (additional information, Supplementary Fig. 6c). Numbers in outlined areas indicate percent CD107a⁺CD3⁺ cells. Data are from one experiment representative of five independent experiments. **c**, Degranulation of ex vivo or expanded CTLs (below plot) in response to HIV-infected macrophages (left), presented relative to their response to HIV-infected CD4⁺ T cells, set as 1 (dashed horizontal line), and of expanded CTLs in response to CEF peptide–loaded macrophages (right). $^{*}P = 0.0036$ (two-sided one sample *t*-test) and $^{**}P < 0.0001$ (two-sided Wilcoxon signed rank test). Data are from five independent experiments with $n = 14$ individual samples (left) or $n = 16$ individual samples (middle) or three independent experiments with $n = 6$ individual samples (right) (one symbol per sample; mean ± s.e.m.). **d**, Flow-cytometry analysis of the expression of IFN-γ by CD107a⁺ ex vivo or expanded CTLs (left margin). Numbers in outlined areas indicate percent IFN-γ⁺CD3⁺ cells. Data are from one experiment representative of five independent experiments. **e**, Expression of IFN-γ by ex vivo or expanded CTLs (below plot) in response to HIV-infected macrophages (left), presented as in **c**, and of expanded CTLs in response to CEF peptide–loaded macrophages (right). $^{*}P = 0.008$ and $^{**}P = 0.0002$ (two-sided one sample *t*-test) and $^{***}P < 0.0001$ (two-sided Wilcoxon signed rank). Data are from five independent experiments with $n = 14$ individual samples (left) or $n = 16$ individual samples (middle) or three independent experiments with $n = 6$ individual samples (right) (one symbol per sample; mean ± s.e.m.). **f**, ELISA of IFN-γ in supernatants of co-cultures of expanded CTLs from HIV⁺ donors (left) or HIV⁻ donors (right), cultured for 18 h with HIV-infected (left) or CEF peptide–loaded (right) target cells (horizontal axis). $^{*}P = 0.0047$ and $^{**}P = 0.0043$ (two-tailed Mann-Whitney test). Data are from two independent experiments with $n = 8$ individual samples (HIV⁺ donors) or three independent experiments with $n = 6$ individual samples (HIV⁻ donors) (one donor per symbol; boxes as in Fig. 2d).

macrophages were recognized similarly, we co-cultured those infected cells with autologous ex vivo or expanded CTLs and measured the frequency of degranulation by surface staining of the lysosome marker CD107a (Fig. 5b). Ex vivo CTLs degranulated similarly in response to infected CD4⁺ T cells and macrophages (Fig. 5c), and the degranulation was HIV specific, since CD8⁺ T cells from HIV⁻ donors did not degranulate (Supplementary Fig. 6c). Peptide-expanded CTLs degranulated significantly more in response to HIV-infected macrophages than in response to CD4⁺ T cells (Fig. 5c). Similar results were obtained for CTLs responding to CEF peptide–loaded target cells (Fig. 5c), which suggested that the enhanced recognition of macrophages compared with that of CD4⁺ T cells was not an HIV-specific phenomenon but was broadly applicable. As described above, the CD107a⁺ CTLs responding to infected CD4⁺ T cells and those responding to macrophages had comparable cytolytic potential, as shown by expression of perforin and granzymes A, B, H, K and M (Supplementary Fig. 5e). Thus, the reduced killing of macrophages was not due to impaired recognition, degranulation or cytolytic potential of the HIV-specific CTLs.

We next investigated whether HIV-infected CD4⁺ T cells and macrophages triggered other CTL effector functions differentially. Effector cells responding to HIV-infected macrophages produced more IFN-γ, as assessed by intracellular cytokine staining, than did those responding to HIV-infected CD4⁺ T cells (Fig. 5d,e). This result was significant for ex vivo CTLs and expanded CTLs. Similar differential responses were observed for CTLs cultured with CEF peptide–loaded target cells (Fig. 5e). The difference in intracellular cytokine staining was also associated with significantly more

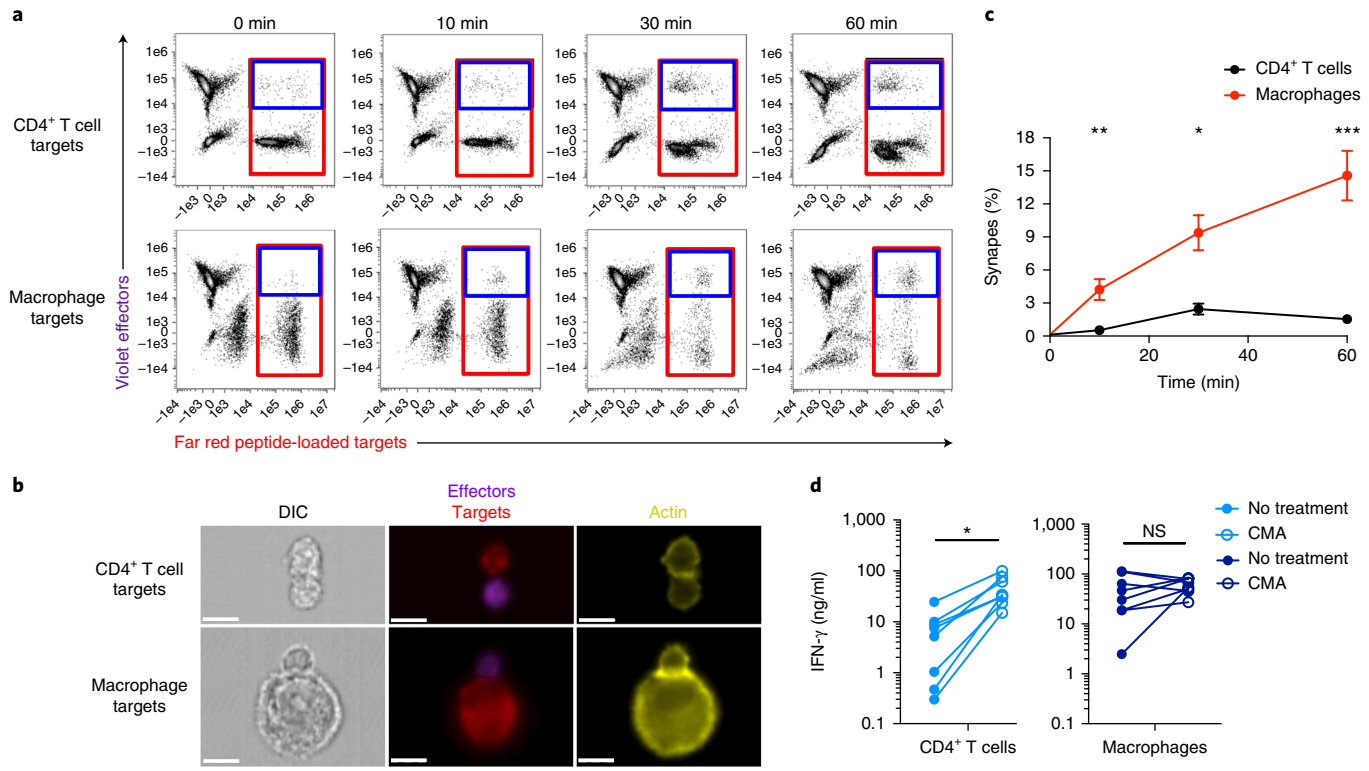


**Fig. 6 | Antigen-loaded macrophages accumulate more immunological synapses with effector cells than do antigen-loaded CD4+ T cells. a**, Imaging-flow-cytometry analysis of expanded CTL effectors (stained with the dye CellTrace Violet) and peptide-loaded, activated CD4+ T cell or macrophage targets (stained with the dye CellTrace Far Red; left margin), assessing doublets after co-culture for various times (above plots), followed by fixation and actin staining; outline colors indicate gating used to quantify total peptide-loaded targets (red) or doublets (blue). Data are from one experiment representative of two independent experiments. **b**, Microscopy identifying immunological synapses between target cells and effector cells in pairs as in **a**, and analysis of concentrated actin (yellow) at the interface between the effector cells and target cells[32] within the doublet gate (far right). Scale bars, 10 μm. DIC, differential interference contrast. Data are from one experiment representative of two independent experiments. **c**, Frequency of immunological synapses over time (horizontal axis) in cells as in **a** (key). $^{*}P = 0.001$, $^{**}P = 0.0001$ and $^{***}P < 0.0001$ (two-sided unpaired *t*-test). Data are from two independent experiments with $n = 6$ individual samples (mean ± s.e.m.). **d**, ELISA of IFN-γ in supernatants of HIV peptide-expanded CTLs pre-incubated for 1 h with CMA or not (No treatment) (key) and then co-cultured for 18 h with HIV-infected CD4+ T cell or macrophage effector cells (horizontal axis). NS, not significant; $^{*}P = 0.0021$ (two-sided paired *t*-test). Data are from two independent experiments with $n = 8$ individual samples (lines connect samples from the same donor).

secreted IFN-γ after overnight co-culture with infected macrophages than after overnight co-culture with infected CD4+ T cell targets, as assessed by ELISA of culture supernatants (Fig. 5f). Approximately tenfold more IFN-γ was released after exposure to infected macrophages than after exposure to CD4+ T cell targets. Again, similar results were obtained for CEF-specific CTLs cultured with CEF peptide–loaded target cells (Fig. 5f). Approximately 4.2-fold more IFN-γ was released after exposure to CEF peptide–loaded macrophages than after exposure to CEF peptide–CD4+ T cell targets. Together these data suggested that CTLs efficiently recognized and produced more cytokine in response to cognate antigen expressed on macrophages than to cognate antigen expressed on CD4+ T cell targets.

**Inefficient killing of macrophages drives enhanced cytokine responses through prolonged effector cell–target cell interactions.** CTLs detach from their specific target cells when the target cell is killed. CTLs that are unable to kill have a prolonged synapse time with the target cell, during which many cytokines, including IFN-γ, are hypersecreted[30]. In addition, children with profound genetic defects in granule-mediated cytotoxicity develop familial hemophagocytic lymphohistiocytosis, an often-fatal syndrome caused by elevated levels of IFN-γ and uncontrolled activation of macrophages[31]. Since CTLs killed macrophages inefficiently (Fig. 1) and produced significantly more IFN-γ after co-culture with macrophages than after co-culture with CD4+ T cells (Fig. 5e,f), we hypothesized that poor killing leads to prolonged synapses between the CTL and macrophage, which drives excessive secretion of IFN-γ. To test our hypothesis, we used imaging flow cytometry to assess, over 1 h, the duration of the formation of synapses between expanded CTL effectors and peptide-loaded activated CD4+ T cell or macrophage targets (Fig. 6a–c). Effector cell–target cell conjugates were distinguished by first gating on total peptide-loaded targets, followed by gating on dually stained effector cell–target cell conjugates (Fig. 6a). The formation of immunological synapses by conjugates was confirmed by assessment of the actin concentration at the cell–cell interface[32] (Fig. 6b). The frequency of effector cell–target cell synapses was low for CD4+ T cells, probably reflective of a short synapse time, whereas macrophages formed a significantly greater frequency of synapses at all time points (Fig. 6c). Although synapse frequency waned after 30 min for CD4+ T cells, they continued to increase for macrophages, which suggested that CTL–macrophage synapses were longer in duration and accumulated over time. Thus, CTLs stayed in contact much longer with macrophage targets than with CD4+ T cells.

To confirm that poor killing and prolonged contact time were responsible for greater cytokine production of CTLs, we assessed

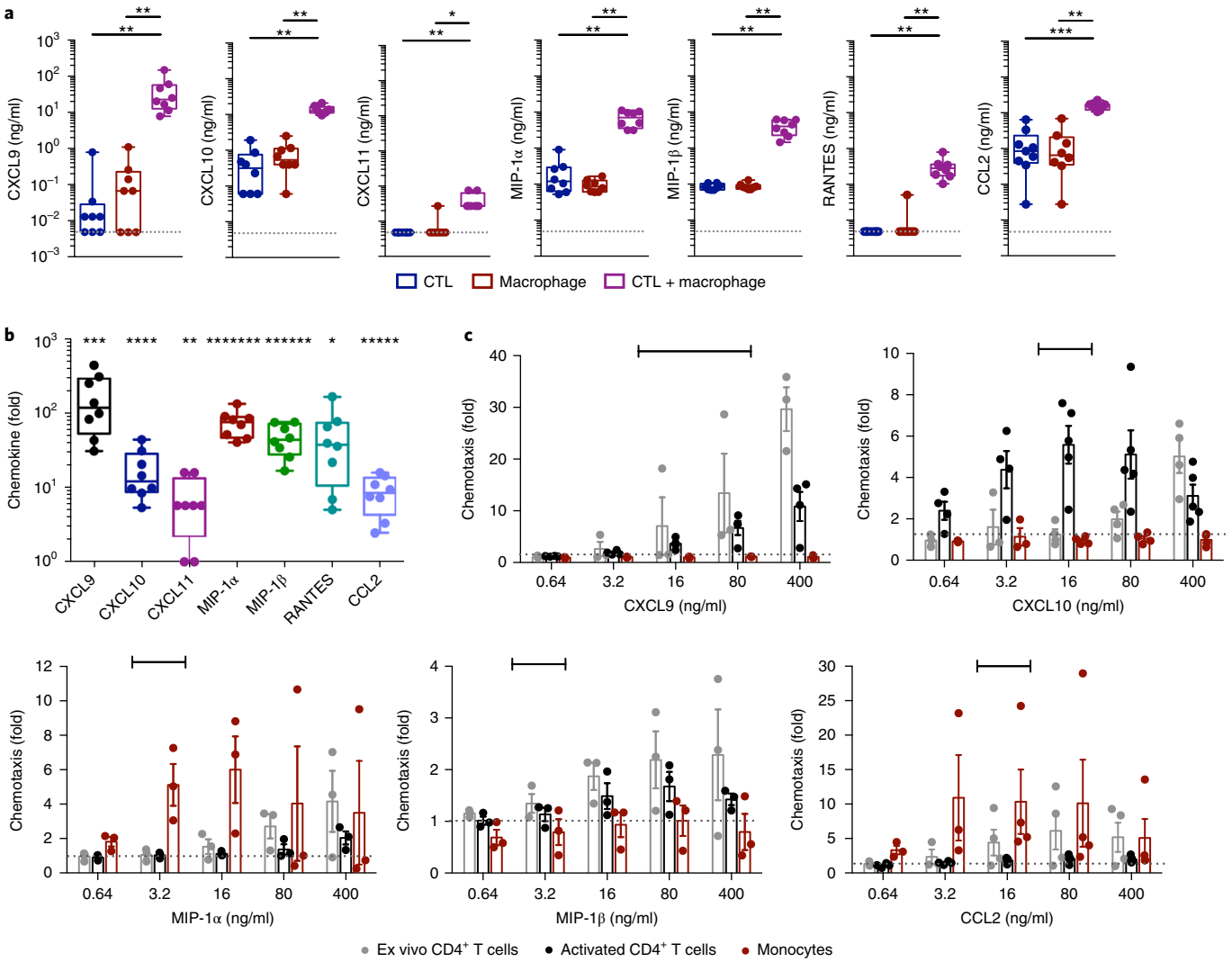


**Fig. 7 | The interaction of CTLs with macrophages induces the production of pro-inflammatory chemokines by macrophages. a**, Cytokine-bead-array analysis of pro-inflammatory chemokines in supernatants of CTLs and/or peptide-loaded macrophages from HIV$^+$ donors, cultured for 24 h alone or together (key); dotted gray line indicates the limit of detection. $^*P = 0.0011$, $^{**}P = 0.0002$ and $^{***}P < 0.0001$ (two-sided Mann-Whitney test). Data are from two independent experiments with $n = 8$ individual samples (one per symbol; boxes as in Fig. 2d). **b**, Production of chemokines (horizontal axis) by CTL-plus-macrophage co-cultures as in **a**, presented relative to that of macrophage-only cultures. $^*P = 0.0286$, $^{**}P = 0.0211$, $^{***}P = 0.0118$, $^{****}P = 0.009$, $^{*****}P = 0.0023$, $^{******}P = 0.0006$ and $^{*******}P = 0.0002$ (two-sided one sample *t*-test). Data are from two independent experiments with $n = 8$ individual samples (one per symbol; boxes as in Fig. 2d). **c**, Chemotaxis of ex vivo CD4$^+$ T cells, activated CD4$^+$ T cells and ex vivo monocytes (key) in response to various concentrations (horizontal axis) of CXCL9, CXCL10, MIP-1α, MIP-1β or CCL2 in a Transwell apparatus (additional information, Supplementary Fig. 7); results are presented as cells that migrated in the presence of the chemokine relative to that in the absence of chemokine. Bracketing above plots indicates the range of chemokine observed in the co-culture conditions in Table 1. Data are from three independent experiments with $n = 3$ individual samples (MIP-1α and MIP-1β) or four independent experiments with $n = 4$ individual samples (CXCL9, CXCL10 and CCL2) (one sample per symbol; mean ± s.e.m.).

whether inhibiting the killing of CD4$^+$ T cells would enhance the secretion of IFN-γ by CTLs exposed to HIV-infected CD4$^+$ T cells. HIV peptide–expanded CTLs that had been given no pre-treatment or had been pre-treated with CMA to inhibit perforin-mediated lysis were cultured overnight with HIV-infected CD4$^+$ T cells or macrophages, followed by measurement of IFN-γ in the culture supernatants. Inhibition of the killing of CD4$^+$ T cells significantly increased the amount of IFN-γ in the supernatants from 7.3 ± 2.8 ng/ml to 46.6 ± 10.4 ng/ml (mean ± s.e.m.), which was comparable to the IFN-γ levels in co-cultures of infected macrophages and untreated CTLs (50.6 ± 15.0 ng/ml) (Fig. 6d). These data suggested that the resistance of macrophages to CTL-mediated killing drove the hypersecretion of IFN-γ.

**CTLs induce the production of pro-inflammatory chemokines by macrophages.** IFN-γ induces the production, by macrophages, of pro-inflammatory chemokines that recruit monocytes and T cells[33–35]. To determine whether the interaction of CTLs with macrophages induced the secretion of pro-inflammatory chemokines, we measured the macrophage-derived chemokines CXCL9, CXCL10, CXCL11, MIP-1α (CCL3), MIP-1β (CCL4), RANTES (CCL5) and CCL2 in culture supernatants after 24 h of co-culture of CTLs and macrophages. Such co-culture resulted in a significant increase in each of the seven chemokines assessed (Fig. 7a). The induction of each of these chemokines in co-cultures relative to their abundance in single cultures was significant (Fig. 7b). In addition, recombinant chemokines added at concentrations measured in those co-cultures

(Table 1) mediated the chemotaxis of T cells (CXCL9, CXCL10, MIP-1β and CCL2) and monocytes (MIP-1α and CCL2) in a Transwell system (Fig. 7c), consistent with the chemokine-receptor profile of each cell type (Supplementary Fig. 7). Together these in vitro results indicated that inefficient killing of macrophages by CTLs might promote the inflammatory chemotaxis of other immune cells.

**Table 1 | Chemokine concentrations in CTL–macrophage co-cultures**

| Chemokine | Concentration (ng/ml) |
|---|---|
| CXCL9 | 42.1 ± 16.5 |
| CXCL10 | 13.7 ± 1.33 |
| CXCL11 | 0.03 ± 0.07 |
| MIP-1α | 7.04 ± 1.28 |
| MIP-1β | 4.07 ± 0.67 |
| RANTES | 0.32 ± 0.07 |
| CCL2 | 15.5 ± 1.33 |

Data are from two independent experiments with $n = 8$ individual samples (mean ± s.e.m.).

## Discussion

Our results have demonstrated that macrophages were inherently more resistant to CTL-mediated killing than were CD4+ T cells. The resistance was associated with less-efficient inhibition of HIV replication by CTLs, prolonged formation of synapses with CTLs and increased secretion of pro-inflammatory cytokines and chemokines. The killing of HIV-infected CD4+ T cells and macrophages was mediated by death-inducing perforin and granzymes from CTLs. However, in contrast to the killing of CD4+ T cells, which was rapid, more effective at suppressing HIV and independent of caspases and granzyme B, the killing of macrophages was slow and caspase dependent and required granzyme B. While our initial observations of differences in the suppression of HIV-infected CD4+ T cells and that of HIV-infected macrophages disagree with one published report[18], potentially due to differences in viral strains, infection protocols, source of CTLs or effector cell/target cell ratios, both that study and ours consistently demonstrated that although killing was delayed, HIV-infected macrophages could be eliminated by CTLs[16,18,19]. Our results agree with and extend results reported for CD4+ T cell and macrophage targets infected with simian immunodeficiency virus[20,21] by demonstrating a mechanism whereby poor killing of target cells induces hyperinflammatory responses[30], which could contribute to chronic inflammation, a hallmark of HIV infection.

Human CTLs can express any combination of five granzymes, each of which activates an independent cell-death pathway. While granzymes B and M induce caspase-dependent apoptosis, granzymes A, H and K are caspase independent[24,26,36,37]. Our results suggested that activated CD4+ T cells might be susceptible to killing by at least one granzyme that induces caspase-independent apoptosis. However, due to a lack of granzyme-specific inhibitors, it is unclear which granzyme was responsible for this killing. The differentiation and activation state of T cells have also been shown to contribute to their susceptibility to rapid killing by CTLs[38]. While we observed no differences between the killing of resting CD4+ T cell targets and that of activated CD4+ T cell targets in our assay, the precise mechanism by which CD4+ T cells are killed remains to be identified. In contrast, macrophages required granzyme B to induce apoptosis through caspase-3-dependent mechanisms and appeared to be resistant to more-rapid, caspase-independent killing. SERPINB9, a natural inhibitor of granzyme B[27], was expressed by both target-cell types. The resistance to granzyme B–mediated apoptosis via SERPINB9 expression in CD4+ T cells was probably overcome by susceptibility to an alternative granzyme that induced apoptosis through a caspase-independent mechanism. In contrast, given that macrophages required granzyme B for their CTL-mediated killing, SERPINB9 expression might slow the initiation of or protect the cell from apoptosis, as noted for Bcl-2[29]. The enhanced resistance of macrophages to CTL-mediated killing might represent a mechanism for preserving antigen presentation and inducing more-potent adaptive immune responses by increasing the survival of antigen-presenting cells, instead of their being killed by sentinel CTLs. In this context, it has been reported that mature dendritic cells are more resistant to lysis by CTLs than are immature dendritic cells[38,39]. We found that macrophages were also resistant to being killed by CMV-, EBV- and Flu-specific CTLs, which would suggest that this resistance and subsequent pro-inflammatory consequences are broadly applicable. Although SERPINB9 represents a mechanism for resisting granzyme B, there are currently no known mechanisms of resistance to the other granzymes. Therefore, understanding how macrophages resist being rapidly killed by a caspase-independent mechanism will require further study.

In this study, we assessed the cytolytic ability of ex vivo CTLs and in vitro–expanded CTLs in the elimination of HIV-infected CD4+ T cells and macrophages. Despite the killing of CD4+ T cells by ex vivo CTLs, the killing of macrophages by ex vivo CTLs was barely detectable, probably due to a combination of the resistance of macrophages to granzymes and the low frequency of perforin-positive, granzyme-positive CTLs. Expanded CTLs, which had higher expression of perforin and granzymes, exhibited greater killing of macrophages; however, as noted for ex vivo CTLs, this was relatively inefficient compared with the killing of CD4+ T cells. As CTLs from HIV controllers maintain their proliferative capacity and express more perforin after restimulation than do those from non-controllers[40], the in vitro–expanded CTLs used in our study probably represent a scenario more physiologically relevant to elite controllers. In contrast, CTLs from HIV+ people with chronic progression of the disease appear to be exhausted and exhibit deficiencies in proliferative ability and low cytolytic potential, but maintain IFN-γ production[41–45]. Indeed, CTLs from such people exhibit poorer killing of both CD4+ T cell targets[46] and macrophage targets[18], and function is not fully restored by combination antiretroviral therapy[47]. Inefficient killing in these contexts might contribute to the persistence of infected macrophages and, potentially, to the chronic inflammatory state observed in all HIV+ patients.

The timing of programmed cell death has consequences. Slow killing by killer lymphocytes in patients bearing hypomorphic *Prf1* mutations results in prolonged interaction of CTLs with their targets and enhanced production of IFN-γ and other pro-inflammatory cytokines[30]. High levels of IFN-γ have been postulated to lie at the root of the often-fatal sequelae of familial hemophagocytic lymphohistiocytosis, as neutralization of this cytokine has been shown to induce recovery in two animal models of this disease[48]. HIV-infected people also experience chronic inflammation[13]. Our results suggest that non-cytolytic interaction of T cells with target cells could potentially contribute to the elevated IFN-γ production and enhanced chronic inflammation in HIV+ patients. For HIV+ patients whose HIV is suppressed with antiretroviral therapy, waning peripheral and tissue T cell responses might prove beneficial in the context of inflammation[49], as less IFN-γ would yield less activation of macrophages. Indeed, markers of chronic inflammation, including soluble CD163 (a monocyte- and macrophage-activation marker), are lower in patients treated with antiretroviral therapy than in elite controllers[50]. IFN-γ-induced activation of macrophages and recruitment of immune cells to sites of infection could contribute to the inflammatory macrophage–associated diseases, including atherosclerosis and neurological disease, that have been reported in HIV+ subjects[11–13].

Our study has suggested that non-cytolytic interactions of CTLs with HIV-infected macrophages might contribute to ongoing inflammatory conditions. Small-animal models of HIV infection are currently inadequate to address the underlying mechanism, due to high levels of background inflammation (graft-versus-host disease) and poor myeloid-cell reconstitution. Future studies with improved small-animal models of HIV infection could help to confirm a causal link between poor killing by CTLs and chronic inflammation. Finally, greater understanding of the precise mechanisms underlying macrophage resistance to target-cell killing and resulting hypersecretion of pro-inflammatory cytokines and chemokines will be needed to develop approaches capable of efficiently eliminating infected macrophages and suppressing excessive inflammation. The inflammatory consequences of poor killing of macrophages might also have implications for other pathogens that infect macrophages, such as *Mycobacterium tuberculosis*, chikungunya virus and adenovirus.

## Methods

Methods, including statements of data availability and any associated accession codes and references, are available at https://doi.org/10.1038/s41590-018-0085-3.

Received: 25 September 2017; Accepted: 13 March 2018;
Published online: 18 April 2018

## References

1. Swingler, S., Mann, A. M., Zhou, J., Swingler, C. & Stevenson, M. Apoptotic killing of HIV-1-infected macrophages is subverted by the viral envelope glycoprotein. *PLoS Pathog.* **3**, 1281–1290 (2007).
2. Groot, F., Welsch, S. & Sattentau, Q. J. Efficient HIV-1 transmission from macrophages to T cells across transient virological synapses. *Blood* **111**, 4660–4663 (2008).
3. Duncan, C. J. et al. High-multiplicity HIV-1 infection and neutralizing antibody evasion mediated by the macrophage-T cell virological synapse. *J. Virol.* **88**, 2025–2034 (2014).
4. Collins, D. R., Lubow, J., Lukic, Z., Mashiba, M. & Collins, K. L. Vpr promotes macrophage-dependent HIV-1 infection of CD4$^+$ T lymphocytes. *PLoS Pathog.* **11**, e1005054 (2015).
5. Honeycutt, J. B. et al. Macrophages sustain HIV replication in vivo independently of T cells. *J. Clin. Invest.* **126**, 1353–1366 (2016).
6. Honeycutt, J. B. et al. HIV persistence in tissue macrophages of humanized myeloid-only mice during antiretroviral therapy. *Nat. Med.* **23**, 638–643 (2017).
7. Avalos, C. R. et al. Quantitation of productively infected monocytes and macrophages of simian immunodeficiency virus-infected macaques. *J. Virol.* **90**, 5643–5656 (2016).
8. Avalos, C. R. et al. Brain Macrophages in simian immunodeficiency virus-infected, antiretroviral-suppressed macaques: a functional latent reservoir. *mBio* **8**, e01186–e01117 (2017).
9. Nowlin, B. T. et al. SIV encephalitis lesions are composed of CD163$^+$ macrophages present in the central nervous system during early SIV infection and SIV-positive macrophages recruited terminally with AIDS. *Am. J. Pathol.* **185**, 1649–1665 (2015).
10. Sattentau, Q. J. & Stevenson, M. Macrophages and HIV-1: an unhealthy constellation. *Cell Host Microbe* **19**, 304–310 (2016).
11. DiNapoli, S. R., Hirsch, V. M. & Brenchley, J. M. Macrophages in progressive human immunodeficiency virus/simian immunodeficiency virus infections. *J. Virol.* **90**, 7596–7606 (2016).
12. Lamers, S. L. et al. HIV-1 Nef in macrophage-mediated disease pathogenesis. *Int. Rev. Immunol.* **31**, 432–450 (2012).
13. Hsu, D. C., Sereti, I. & Ananworanich, J. Serious non-AIDS events: immunopathogenesis and interventional strategies. *AIDS Res. Ther.* **10**, 29 (2013).
14. Streeck, H. & Nixon, D. F. T cell immunity in acute HIV-1 infection. *J. Infect. Dis.* **202**(Suppl 2), S302–S308 (2010).
15. Goulder, P. J. & Walker, B. D. The great escape — AIDS viruses and immune control. *Nat. Med.* **5**, 1233–1235 (1999).
16. Fujiwara, M. & Takiguchi, M. HIV-1-specific CTLs effectively suppress replication of HIV-1 in HIV-1-infected macrophages. *Blood* **109**, 4832–4838 (2007).
17. Severino, M. E. et al. Inhibition of human immunodeficiency virus type 1 replication in primary CD4$^+$ T lymphocytes, monocytes, and dendritic cells by cytotoxic T lymphocytes. *J. Virol.* **74**, 6695–6699 (2000).
18. Walker-Sperling, V. E., Buckheit, R. W. III & Blankson, J. N. Comparative analysis of the capacity of elite suppressor CD4$^+$ and CD8$^+$ T cells to inhibit HIV-1 replication in monocyte-derived macrophages. *J. Virol.* **88**, 9789–9798 (2014).
19. Walker-Sperling, V. E. et al. Short communication: HIV controller T cells effectively inhibit viral replication in alveolar macrophages. *AIDS Res. Hum. Retroviruses* **32**, 1097–1099 (2016).
20. Rainho, J. N. et al. Nef Is dispensable for resistance of simian immunodeficiency virus-infected macrophages to CD8$^+$ T cell killing. *J. Virol.* **89**, 10625–10636 (2015).
21. Vojnov, L. et al. The majority of freshly sorted simian immunodeficiency virus (SIV)-specific CD8. T cells cannot suppress viral replication in SIV-infected macrophages. *J. Virol.* **86**, 4682–4687 (2012).
22. Walker, B. D. & Yu, X. G. Unravelling the mechanisms of durable control of HIV-1. *Nat. Rev. Immunol.* **13**, 487–498 (2013).
23. Slee, E. A., Adrain, C. & Martin, S. J. Executioner caspase-3, -6, and -7 perform distinct, non-redundant roles during the demolition phase of apoptosis. *J. Biol. Chem.* **276**, 7320–7326 (2001).
24. Lieberman, J. The ABCs of granule-mediated cytotoxicity: new weapons in the arsenal. *Nat. Rev. Immunol.* **3**, 361–370 (2003).
25. Belizario, J., Vieira-Cordeiro, L. & Enns, S. Necroptotic cell death signaling and execution pathway: lessons from knockout mice. *Mediators Inflamm.* **2015**, 128076 (2015).
26. Lieberman, J. Cell-mediated cytotoxicity. in *Fundamental Immunology* (ed. Paul, W.E.) 7th edn (Lippincott Williams & Wilkins, Philadelphia, 2013).
27. Kaiserman, D. & Bird, P. I. Control of granzymes by serpins. *Cell Death Differ.* **17**, 586–595 (2010).
28. Kataoka, T. et al. Concanamycin A, a powerful tool for characterization and estimation of contribution of perforin- and Fas-based lytic pathways in cell-mediated cytotoxicity. *J. Immunol.* **156**, 3678–3686 (1996).
29. Sutton, V. R. et al. Granzyme B triggers a prolonged pressure to die in Bcl-2 overexpressing cells, defining a window of opportunity for effective treatment with ABT-737. *Cell Death Dis.* **3**, e344 (2012).
30. Jenkins, M. R. et al. Failed CTL/NK cell killing and cytokine hypersecretion are directly linked through prolonged synapse time. *J. Exp. Med.* **212**, 307–317 (2015).
31. Stepp, S. E. et al. Perforin gene defects in familial hemophagocytic lymphohistiocytosis. *Science* **286**, 1957–1959 (1999).
32. Calabia-Linares, C. et al. Endosomal clathrin drives actin accumulation at the immunological synapse. *J. Cell Sci.* **124**, 820–830 (2011).
33. Corbera-Bellalta, M. et al. Blocking interferon γ reduces expression of chemokines CXCL9, CXCL10 and CXCL11 and decreases macrophage infiltration in ex vivo cultured arteries from patients with giant cell arteritis. *Ann. Rheum. Dis.* **75**, 1177–1186 (2016).
34. Foley, J. F. et al. Roles for CXC chemokine ligands 10 and 11 in recruiting CD4$^+$ T cells to HIV-1-infected monocyte-derived macrophages, dendritic cells, and lymph nodes. *J. Immunol.* **174**, 4892–4900 (2005).
35. Reinhart, T. A. et al. Increased expression of the inflammatory chemokine CXC chemokine ligand 9/monokine induced by interferon-? in lymphoid tissues of rhesus macaques during simian immunodeficiency virus infection and acquired immunodeficiency syndrome. *Blood* **99**, 3119–3128 (2002).
36. de Poot, S. A. et al. Granzyme M targets topoisomerase II alpha to trigger cell cycle arrest and caspase-dependent apoptosis. *Cell Death Differ.* **21**, 416–426 (2014).
37. Ewen, C. L., Kane, K. P. & Bleackley, R. C. Granzyme H induces cell death primarily via a Bcl-2-sensitive mitochondrial cell death pathway that does not require direct Bid activation. *Mol. Immunol.* **54**, 309–318 (2013).
38. Liu, J. & Roederer, M. Differential susceptibility of leukocyte subsets to cytotoxic T cell killing: implications for HIV immunopathogenesis. *Cytometry A* **71**, 94–104 (2007).
39. Medema, J. P. et al. Expression of the serpin serine protease inhibitor 6 protects dendritic cells from cytotoxic T lymphocyte-induced apoptosis: differential modulation by T helper type 1 and type 2 cells. *J. Exp. Med.* **194**, 657–667 (2001).
40. Migueles, S. A. et al. HIV-specific CD8$^+$ T cell proliferation is coupled to perforin expression and is maintained in nonprogressors. *Nat. Immunol.* **3**, 1061–1068 (2002).
41. Wherry, E. J. T cell exhaustion. *Nat. Immunol.* **12**, 492–499 (2011).
42. Hersperger, A. R. et al. Perforin expression directly ex vivo by HIV-specific CD8 T-cells is a correlate of HIV elite control. *PLoS Pathog.* **6**, e1000917 (2010).
43. Trimble, L. A. & Lieberman, J. Circulating CD8 T lymphocytes in human immunodeficiency virus-infected individuals have impaired function and downmodulate CD3 zeta, the signaling chain of the T-cell receptor complex. *Blood* **91**, 585–594 (1998).
44. Draenert, R. et al. Persistent recognition of autologous virus by high-avidity CD8 T cells in chronic, progressive human immunodeficiency virus type 1 infection. *J. Virol.* **78**, 630–641 (2004).
45. Appay, V. et al. HIV-specific CD8$^+$ T cells produce antiviral cytokines but are impaired in cytolytic function. *J. Exp. Med.* **192**, 63–75 (2000).

46. Migueles, S. A. et al. Lytic granule loading of CD8+ T cells is required for HIV-infected cell elimination associated with immune control. *Immunity* **29**, 1009–1021 (2008).
47. Migueles, S. A. et al. Defective human immunodeficiency virus-specific CD8+ T-cell polyfunctionality, proliferation, and cytotoxicity are not restored by antiretroviral therapy. *J. Virol.* **83**, 11876–11889 (2009).
48. Pachlopnik Schmid, J. et al. Neutralization of IFNγ defeats haemophagocytosis in LCMV-infected perforin- and Rab27a-deficient mice. *EMBO Mol. Med.* **1**, 112–124 (2009).
49. Critchfield, J. W. et al. Magnitude and complexity of rectal mucosa HIV-1-specific CD8+ T-cell responses during chronic infection reflect clinical status. *PLoS One* **3**, e3577 (2008).
50. Pereyra, F. et al. Increased coronary atherosclerosis and immune activation in HIV-1 elite controllers. *AIDS* **26**, 2409–2412 (2012).

## Acknowledgements

We thank S. Buus (University of Copenhagen) for monomers; G. Mylvaganam, G. Gaiha, T. Diefenbach and A. Balazs for comments; J. Trapani for discussions about granzymes; A. Piechocka-Trocha for experimental help; and the Flow Cytometry and Sample Processing Cores at the Ragon Institute for help with instrumentation and processing of the samples. Supported by the Howard Hughes Medical Institute (D.R.C. and B.D.W.), the Ragon Institute of MGH, MIT and Harvard (B.D.W.), the Canadian Institute of Health Research (K.L.C.), the US National Institutes of Health (R01 AI118544 to B.D.W.), amfAR (109326-59-RGRL to K.L.C. and B.D.W.) and the Harvard University Center for AIDS Research (P30 AI060354 to B.D.W.), which is supported by the following institutes and centers co-funded by and participating with the US National Institutes of Health: NIAID, NCI, NICHD, NHLBI, NIDA, NIMH, NIA, FIC and OAR.

## Author contributions

K.L.C. designed and performed the experiments and wrote the manuscript; D.R.C and B.D.W. contributed to the design of the experiments and writing of the manuscript; J. Lengieza performed experiments and optimized macrophage infection conditions; M.G provided advice for statistical analysis; F.D contributed to the discussions of granzyme-induced cell-death experiments; J. Lieberman provided guidance and design for apoptosis, granzyme and perforin experiments and for editing of the manuscript; and B.D.W. provided overall supervision of the project.

## Competing interests

The authors declare no competing interests.

## Additional information

**Supplementary information** is available for this paper at https://doi.org/10.1038/s41590-018-0085-3.

**Reprints and permissions information** is available at www.nature.com/reprints.

**Correspondence and requests for materials** should be addressed to B.D.W.

**Publisher's note:** Springer Nature remains neutral with regard to jurisdictional claims in published maps and institutional affiliations.

## Methods

**Human subjects.** HIV$^+$ subjects were recruited from outpatient clinics at local Boston area clinics and from outside Boston. The institutional review board of Massachusetts General Hospital approved the studies of cells derived from human blood samples. All human subjects gave written, informed consent. Peripheral blood mononuclear cells (PBMCs) from healthy HIV$^-$donors and HIV$^+$ controllers were collected by Ficoll gradient separation from leukapheresis samples, then were cryopreserved and stored at −150 °C for future use. Controller status was classified as previously described[51].

**Cell isolation and culture.** For preparation of target cells, frozen PBMCs were thawed and subjected to CD14 positive isolation (Stemcell Technologies) per the manufacturer's instructions to isolate monocytes. CD4$^+$ T cells were isolated via negative enrichment (Stemcell Technologies) using the leftover CD14-depleted PBMCs. Macrophages were obtained via 7-day maturation of monocytes with 50 ng/ml recombinant human GM-CSF (BioLegend) and 50 ng/ml recombinant human M-CSF (BioLegend) in R10 medium (RPMI 1640, 10% FBS, 1 U/ml penicillin, 100 mg/ml streptomycin, 2 mM glutamine and 10 mM HEPES; Sigma) in low-attachment 24-well plates (400,000 cells per well; Corning). In addition, different lots of 'Certified FBS' (Invitrogen) were screened for the best induction of macrophage maturation that yielded efficient levels of HIV infection. Half of the maturation medium was exchanged for fresh medium containing GM-CSF and M-CSF on day 4. Alternative methods to obtain macrophages included maturation using 10% Human Serum AB (Gemini Bio-Products; Supplementary Fig. 3a only). Successful maturation was assessed via spreading of the cells onto the surface of the plate[4]. CD4$^+$ T cells were rested overnight in R10 with 30 U/ml IL-2 (R10/30; NIH AIDS Reagent Program), then were activated using plate-bound anti-CD3 (clone OKT3; BioLegend) and soluble anti-CD28 (clone 28.8; BioLegend) in R10/30 to permit HIV infection. After three days of activation, cells were removed from the plate and rested in R10/30 for an additional 3 d before infection. For experiments using resting ex vivo CD4$^+$ T cells (Supplementary Fig. 3), CD4$^+$ T cells were isolated from frozen PBMCs immediately before co-culture with CTL effectors.

For preparation of ex vivo effector cells, autologous PBMCs were thawed and rested in R10 medium with 5 U/ml recombinant IL-2 (R10/5) for 8–10 h before co-culture with target cells. CD8$^+$ T cells were isolated via negative enrichment (Stemcell Technologies), followed by CD62L depletion (Miltenyi) per the manufacturer's instructions. This negative enrichment kit contains antibodies to CD56 and CD16 to effect depletion of natural killer cells. For preparation of HIV peptide–expanded and CMV, EBV, and Flu (CEF) peptide–expanded effector cells, autologous PBMCs were thawed 3 d before co-culture and were stimulated in R10 with 50 U/ml IL-2 (R10/50) and 200 ng/ml/peptide of a pool of HIV or CEF peptides representing optimal MHC class I–restricted epitopes matched for each subject's HLA type. PBMCs from healthy HIV$^-$ donors were stimulated with 0.5 μg/ml of anti-CD3 and anti-CD28 (identified above) for negative controls in elimination assays. 7 d following activation, effector CTLs were isolated as described above and rested in R10/50 for an additional 5 d before use in co-culture assays.

**Preparation of HIV stocks.** HEK293T17 cells (obtained from ATCC; cells were not tested for mycoplasma) were transfected with 89.6 or JR-CSF proviral plasmid (NIH AIDS Reagent Program) using 25-kDa polyethylenimine (PEI; Polysciences). At 40–48 h after transfection, culture supernatants were collected, centrifuged at 3,000 *g* for 10 min to remove cell debris, filtered through a 0.45-μm membrane to remove smaller aggregates and concentrated with PEG-it Virus Precipitation Solution (System Biosciences) according to the manufacturer's instructions and were frozen at −80 °C. Viral stocks were titered via p24 ELISA (Frederick National Laboratory for Cancer Research).

**Preparation of HIV-infected target cells.** $HIV_{89.6}$, an R5X4 dual-tropic strain, was used to infect GM-CSF- and M-CSF-derived macrophages and CD4$^+$ T cells for co-culture assays. $HIV_{JRCSF,}$ an R5 strain, was used for assays containing human serum–derived macrophages and CD4$^+$ T cells. For $HIV_{JRCSF}$ experiments, macrophages were pre-transduced with SIV Vpx for 24 h to enhance HIV infection (Supplementary Fig. 3a). Macrophages and CD4$^+$ T cells were infected as previously described[4]. Macrophages were incubated for 6 h at 37 °C with 100 ng p24 of $HIV_{89.6}$ in each well of a 24-well plate, followed by removal of the virus. In parallel, activated CD4$^+$ T cells were infected in 96-well flat-bottom plates at $1 \times 10^6$ cells per well with 40 ng p24 of $HIV_{89.6}$ and were spin-inoculated at 800 *g* for 1 h and incubated at 37 °C for 3 h, followed by removal of the virus. 2 d following initial infection with HIV, levels of infection were assessed for each target cell via flow cytometry before setting up of co-culture assays. Macrophages or CD4$^+$ T cells were surface stained with anti-CD14-APC/Cy7 (clone M5E2; BioLegend) or anti-CD3-APC/Cy7 (clone HIT3a; BioLegend), respectively, and anti-CD4-APC (clone OKT4; BioLegend) and LIVE/DEAD Blue (ThermoFisher), followed by intracellular staining with anti-Gag p24-RD1 (clone KC-57; Beckman Coulter). Intracellular staining for SERPINB9 was performed using anti-SERPINB9-AF488 (PI-9, clone 7D8; BioRad). Flow-cytometry data were acquired using a FACSCanto instrument with FACSDiva software (BD Biosciences). Uninfected cells were added to normalize infection levels between the two target cell types. Target cell infection ranged from 2.0% to 16.6% in elimination, suppression and recognition assays.

**Preparation of peptide-loaded target cells.** For assays using peptide-loaded targets, uninfected, activated CD4$^+$ T cells or macrophages were incubated for 30 min at 37 °C with 1 μg/ml per peptide of the HIV or CEF optimal peptides used to make their autologous expanded CTLs. Where indicated, resting CD4$^+$ T cells (unstimulated, total ex vivo CD4$^+$ T cells) were used in place of activated CD4$^+$ T cells. During the final 5 min of incubation, CellTrace FarRed (ThermoFisher) was added to the culture. Cells were washed twice in R10 and then mixed 1:1 with unloaded, unlabeled target cells, producing a population of 50% peptide-loaded target cells. These targets were used for elimination, recognition and conjugate- or synapse-formation assays.

**Tetramer staining and perforin–granzyme phenotyping of ex vivo CD8$^+$ T cells.** Rested ex vivo CD8$^+$ T cells were assessed for CMV and HIV specificity using HLA-matched tetramers. Tetramers were made via biotinylated monomer conjugation to BV510 streptavidin (BioLegend). Monomers were obtained from S. Buus (University of Copenhagen). The A02-NV9 tetramer was used to stain for CMV-specificity while pools of A02-SL9, B27-KK10, B53-QW9, B53-YY9, B57-IW9(p24), B57-IW9(RT), B57-KF11, B57-QW9 and B57-TW10 tetramers were used to stain for HIV specificity. Subsequent surface stains included anti-CD62L-PE-Cy5 (clone DREG-56; BioLegend), anti-CD3-AF700 (clone HIT3a; BioLegend), anti-CD8-FITC (clone SK1; BioLegend), anti-CD45RA-BV605 (clone HI100; BioLegend) and LIVE/DEAD Blue. Following permeabilization, the cells were intracellular stained using anti-perforin PE/Cy7 (clone B-D48; BioLegend), anti-granzyme A-PerCp/Cy5.5 (clone CB9; BioLegend), anti-granzyme B-Pacific Blue (clone GB11; BioLegend), anti-granzyme H (biotinylated and secondary stained with BV650 streptavidin) (catalog# BAF1377, R&D), anti-granzyme K-PE (clone GM26E7; BioLegend), and anti-granzyme M-eFluor660 (clone 4B2G4; eBioscience). The cells were analyzed by flow cytometry. Naïve CD8$^+$ T cells within the mixed population of CD8$^+$ T cells were used as internal gating controls for perforin and each granzyme as these cells do not express these effector molecules.

**CTL elimination assay.** Infected or peptide-loaded CD4$^+$ T cell and macrophage target cells and effector CTLs (ex vivo and peptide expanded) were prepared as described above. Effector cells were stained with CellTrace Violet (ThermoFisher) to distinguish target cells and effector cells via flow cytometry. For assays assessing inhibition of killing, effector cells were pre-incubated with 100 ng/ml of concanamycin A[28,52] (Tocris), 100 μM granzyme B inhibitor II[53] (Millipore), 2 μg/ml anti-FAS[52] (clone ZB4; Millipore) or 1 μg/ml TRAIL-R1–Fc[54] (R&D), while target cells were pre-incubated with 50 μM necrostatin-1 (Millipore), 100 μM caspase inhibitor I (pan-caspase inhibitor; Millipore), 100 μM caspase-3 inhibitor (R&D) or 80 μg/ml of antibody to MHC class I (clone W6/32; BioLegend). Isotype-matched control antibody and vehicle controls were included for comparison. Effector cells were co-cultured with mock-treated, peptide-loaded or infected target cells at an effector cell/target cell ratio of 0, 1, 2, and 4 for 4 h (or for 15 min, 1 h, 4 h, 12 h and 24 h for the time course) at 37 °C. During the final hour of incubation, a fixable fluorescent inhibitor of caspase-3 (FAM-DEVD-FMD; ThermoFisher) or the ROS-detection reagent CellROX (ThermoFisher) was added, as indicated. Cells were harvested and surface stained with anti-CD14-APC/Cy7 (for macrophages) (clone M5E2; BioLegend) or anti-CD3-APC/Cy7 (for CD4$^+$ T cells) (clone HIT3a; BioLegend), in addition to anti-CD4-APC (for infected target cells only) (clone OKT4; BioLegend) and LIVE/DEAD Blue (ThermoFisher), followed by intracellular staining with anti-Gag p24-RD1 (for infected targets only) (clone KC-57; Beckman Coulter) and flow cytometry.

**Calculations for elimination assay analysis.** Elimination of infected target cells was assessed via quantitation of live (LIVE/DEAD Blue–negative) CD4$^-$p24$^+$ target cells, while early apoptotic LIVE/DEAD-negative CD4$^-$p24$^+$ target cells were detected via induction of active caspase-3 or ROS activity. The percentage of residual Gag$^+$ targets was calculated by division of the percentage of CD4$^-$p24$^+$ cells at an effector cell/target cell ratio of 1, 2 or 4 by the percentage of CD4$^-$p24$^+$ cells at an effector cell/target cell ratio of 0, followed by multiplication of the result by 100. Casapse-3 activity was calculated by subtraction of percentage of cells with active caspase-3 at an effector cell/target cell ratio of 0 from the percentage of cells with active caspase-3 at an effector cell/target cell ratio of 4. ROS activity was calculated by subtraction of the percentage of cells expressing ROS at an effector cell/target cell ratio of 0 from the percentage of cells expressing ROS at an effector cell/target cell ratio of 2. Elimination of peptide-loaded target cells was assessed via the loss of LIVE/DEAD Blue–negative, Far Red$^+$ target cells. Percent residual peptide-loaded targets was calculated by division of the percentage of Far Red$^+$ targets at an effector cell/target cell ratio of 1, 2 or 4 by the percentage of Far Red$^+$ targets at an effector cell/target cell ratio of 0, followed by multiplication of the result by 100.

**Viral inhibition assay.** Infected CD4$^+$ T cells, macrophages and ex vivo CTLs were prepared as described above. Co-cultures were performed in 96-well plates in 200 μl of R10/50 at an effector cell/target cell ratio of 2. On days three, five, and seven of co-culture, 100 μl of culture supernatant was harvested and replaced with 100 μl of new R10/50. Quantitation of virus in the culture supernatants was performed using p24 ELISA (NCI Frederick). The percentage of viral suppression was calculated by subtraction of the p24 concentration at an effector cell/target cell ratio of 2 from

that at a paired effector cell/target cell ratio of 0, division of the p24 concentration at an effector cell/target cell ratio of 0 and multiplication of the result by 100.

**Recognition assay.** For flow cytometry-based recognition assays, infected or peptide-loaded CD4+ T cells and macrophages were prepared as described above, followed by co-culture with ex vivo or peptide-expanded CTLs at an effector cell/target cell ratio of 2 in the presence of GolgiPlug/GolgiStop (BD Biosciences) and anti-CD107a-AF488 (clone H4A3; BioLegend). Following 6 h of incubation at 37 °C, cells were harvested and surface stained with anti-CD62L-PE-Cy5 (clone DREG-56; BioLegend), anti-CD3-APC/Cy7 (clone HIT3a; BioLegend), anti-CD8-AF700 (clone SK1; BioLegend), anti-CD45RA-BV650 (clone HI100; BioLegend) and LIVE/DEAD Blue. Intracellular staining was performed using anti-IFN-γ -BV510 (clone 4 S.B3; BioLegend), and cells were analyzed by flow cytometry. For perforin–granzyme phenotyping of degranulated cells, the perforin–granzyme-staining panel described above was used, with anti-IFN-γ-BV510 replacing the tetramer-BV510 stain, anti-CD3-BUV395 (clone HIT3a; BD Biosciences) replacing anti-CD3-AF700, and anti-CD8-AF700 (clone SK1; BioLegend) replacing anti-CD8-FITC.

For ELISA-based recognition assays, effector cell–target cell co-cultures were set up as described above without GolgiPlug/GolgiStop or CD107a-AF488 for an overnight co-culture to allow accumulation of IFN-γ and chemokines. For inhibition of target-cell killing, effector cells were pre-incubated with DMSO or 100 ng/ml CMA for 1 h. At 18 h following co-culture, 100 µl of culture supernatant was collected and IFN-γ levels were assessed via ELISA (BioLegend). For quantitation of chemokine, peptide-loaded macrophages and expanded effector CTLs were cultured individually or were co-cultured at an effector cell/target cell ratio of 2 (150,000 target cells per well or 300,000 CTLs per well) in 24-well plates in R10/50 for 24 h at 37 °C. 100 µl of culture supernatant was collected for cytokine-bead-array measurement of CXCL9, CXCL10, CXCL11, MIP-1α, MIP-1β and CCL2 (LEGENDPlex, BioLegend).

**Calculations for the recognition assay analysis.** CD107a+ cell frequencies were corrected for the background frequencies observed in mock conditions. For samples with infected target cells, CD107a+ cell frequencies were also normalized to the productive infection of CD4+ T cells. The final analysis of degranulation is presented as the CTL response to macrophages relative to the CTL response to CD4+ T cells. Only samples showing at least a 1% CD107a response over mock background for either paired CD4+ T cells or macrophages were included in the analysis. For assessment of effector response quality, frequencies of IFN-γ were assessed in CD107a+ CTLs. The final analysis of IFN-γ was expressed as the CTL fold response to macrophages over CD4+ T cells. For ELISA-based recognition assays, levels of IFN-γ were normalized to productive infection of CD4+ T cells, as described for normalization of CD107a+ cell frequencies.

**Imaging flow cytometry (ImageStream) assay.** For assessment of MHC class I surface density, activated CD4+ T cells and macrophages were harvested and stained with anti-MHC class I-BV510 (clone W6/32; BioLegend) and LIVE/DEAD Near-IR (Invitrogen), followed by fixation and intracellular staining for actin using Phalloidin-AF555 (Invitrogen). 5,000–10,000 events were collected from each sample on the ImageStream X Mark II imaging flow cytometer (Amnis) and were analyzed using IDEAS Software (Millipore). Events in focus were gated, followed by that of cells with an actin staining aspect ratio of 0.9–1.0, which represents cells with near circular morphology. Live cells were gated, followed by assessment MHC class I mean fluorescence intensity (MFI) and cell height (diameter in µm). 'Corrected' MFI was calculated by subtracting the MFI of the fluorescence minus one (FMO) staining control from the MHC class I-BV510–stained sample. Surface area was calculated via the diameter of the cells using the following formula: surface area $= \pi \times (\text{diameter})^2$. Thus, relative surface density of MHC class I for both cell types was calculated by division of the corrected MFI of MHC class I by the surface area.

For the conjugate-synapse-formation assay, peptide-loaded CD4+ T cells, macrophages and expanded effector CTLs were co-cultured at an effector cell/target cell ratio of 2 in 96-well round bottom plates at $30 \times 10^6$ cells per ml in R10/50 for 0, 10, 30 or 60 min at 37 °C, then 100 µl of 4% paraformaldehyde was added directly to the cells at 4 °C for 15 min. Cells were washed, permeabilized and stained with Phalloidin-AF555 (Invitrogen) for actin staining. 50,000 events were collected from each sample on the ImageStream X Mark II imaging flow cytometer and were analyzed using IDEAS Software. The frequency of immunological synapses was calculated by division of the number of conjugates (effector cell–target cell pairs) with immunological synapses (concentrated actin at the cell-cell interface[32]) by the total number of Far Red+ peptide-loaded targets for each time point.

**Chemotaxis assay.** CD4+ T cells were activated as describe above for HIV infection, and rested for 3 d in R10/50. CD4+ T cells and monocytes were isolated from PBMCs as described above to obtain ex vivo cells. All three cell types were resuspended to $2.6 \times 10^6$ cells per ml in R10, and 75 µl was plated onto 3.0-µm pore polycarbonate membranes of a HTS transwell 96-well plate (Corning). Recombinant human chemokines CXCL9, CXCL10, MIP-1α, MIP-1β and CCL2 (BioLegend) were titered from 400 ng/ml to 0.64 ng/ml in R10. 235 µl of each chemokine concentration was plated in the lower wells of the Transwell plate. The membrane support containing the cells was then lowered onto the bottom chamber containing the chemokine medium, followed by incubation at 37 °C for 1.5 h. The membrane support was carefully removed and the medium was transferred to a 96-well round-bottom plate and centrifuged to pellet the cells. 135 µl of medium was removed, 100 µl of CellTiter-Glo 2.0 Assay reagent (Promega) was mixed with the remaining medium, and bioluminescence readings were taken in black 96-well plates (Corning). In parallel, a standard curve was created for each cell type, with top cell numbers per well of 200,000 and tenfold dilutions down to 20. Bioluminescence readings from the cell dilutions were used to create a standard curve to allow calculation of the number of cells that migrated to the lower chamber of each well. Each cell type was also phenotyped for chemokine receptor expression with anti-CD4-AF488 (clone OKT4; BioLegend), anti-CCR2-PE (clone K036C2; BioLegend), anti-CD3-APC/Cy7 (clone HIT3a; BioLegend), anti-CD14-AF700 (clone M5E2; BioLegend), anti-CXCR3-AF647 (clone G025H7; BioLegend), and anti-CCR5-Pacific Blue (clone J418F1; BioLegend) and LIVE/DEAD Blue (ThermoFischer).

**Statistical analysis.** The data were summarized using descriptive measures such as mean, s.d., median, inter quartile range (IQR), frequency and percent (%). Statistical tests such as one-sample, two-sample and paired *t*-tests and their non-parametric alternatives (Wilcoxon signed rank, Mann-Whitney and Wilcoxon matched-pairs signed rank) were used to compare outcome variables. Normality was assessed using diagnostic plots (for example, histogram, box and normal probability plots) and statistical tests (for example, skewness, kurtosis and Shapiro-Wilks). All *P* values are two-sided, and $P < 0.05$ was considered significant. Statistical analysis and graphing were performed using GraphPad Prism 6.0.

**Reporting Summary.** Further information on experimental design is available in the Nature Research Reporting Summary linked to this article.

**Data availability.** The data that support the findings of this study, as well as the datasets generated and/or analyzed during this study, are available from the corresponding author upon request. All data generated or analyzed during this study are included in this published article (and its supplementary information files). All figures have associated raw data.

## References


51. Pereyra, F. et al. HIV control is mediated in part by CD8+ T-cell targeting of specific epitopes. *J. Virol.* **88**, 12937–12948 (2014).
52. Salerno-Goncalves, R., Fernandez-Vina, M., Lewinsohn, D. M. & Sztein, M. B. Identification of a human HLA-E-restricted CD8+ T cell subset in volunteers immunized with *Salmonella enterica* serovar Typhi strain Ty21a typhoid vaccine. *J. Immunol.* **173**, 5852–5862 (2004).
53. Metkar, S. S. et al. Granzyme B activates procaspase-3 which signals a mitochondrial amplification loop for maximal apoptosis. *J. Cell Biol.* **160**, 875–885 (2003).
54. Bellucci, R. et al. Tyrosine kinase pathways modulate tumor susceptibility to natural killer cells. *J. Clin. Invest.* **122**, 2369–2383 (2012).

nature research

Corresponding author(s): Bruce D. Walker

# Life Sciences Reporting Summary

Nature Research wishes to improve the reproducibility of the work that we publish. This form is intended for publication with all accepted life science papers and provides structure for consistency and transparency in reporting. Every life science submission will use this form; some list items might not apply to an individual manuscript, but all fields must be completed for clarity.

For further information on the points included in this form, see Reporting Life Sciences Research. For further information on Nature Research policies, including our data availability policy, see Authors & Referees and the Editorial Policy Checklist.

Please do not complete any field with "not applicable" or n/a. Refer to the help text for what text to use if an item is not relevant to your study.
For final submission: please carefully check your responses for accuracy; you will not be able to make changes later.

## Experimental design

1. Sample size

   Describe how sample size was determined.

   Sample sizes were determined based on availability and resource, and this allowed us to detect statistically significant differences in study variables with adequate power. All sample sizes as well as statistical methods and p values are indicated in the Figure Legends.

2. Data exclusions

   Describe any data exclusions.

   For recognition assays, only samples showing at least 1% CD107a response over mock background for either paired CD4+T cell or macrophages were included in the analysis (Methods section, paragraph 13)

3. Replication

   Describe the measures taken to verify the reproducibility of the experimental findings.

   In order to ensure that the data could be reliably produced, multiple replicates were performed for each experiment. This is expressed in the figure legends. All attempts at experimental replication were successful

4. Randomization

   Describe how samples/organisms/participants were allocated into experimental groups.

   People were randomized based on whether or not they had HIV infection. Infection status was determined by antibody ELISA.

5. Blinding

   Describe whether the investigators were blinded to group allocation during data collection and/or analysis.

   All studies were performed in vitro. Blinding was not performed for this study as the knowledge of patient HIV status was required for selection of samples for HIV-elimination and recognition assays. In addition, HLA status was required for generation of short-term peptide-stimulated cell lines.

Note: all in vivo studies must report how sample size was determined and whether blinding and randomization were used.

6. Statistical parameters

For all figures and tables that use statistical methods, confirm that the following items are present in relevant figure legends (or in the Methods section if additional space is needed).

| n/a | Confirmed |
|---|---|
| ☐ | ☒ The exact sample size (*n*) for each experimental group/condition, given as a discrete number and unit of measurement (animals, litters, cultures, etc.) |
| ☐ | ☒ A description of how samples were collected, noting whether measurements were taken from distinct samples or whether the same sample was measured repeatedly |
| ☐ | ☒ A statement indicating how many times each experiment was replicated |
| ☐ | ☒ The statistical test(s) used and whether they are one- or two-sided<br>*Only common tests should be described solely by name; describe more complex techniques in the Methods section.* |
| ☒ | ☐ A description of any assumptions or corrections, such as an adjustment for multiple comparisons |
| ☐ | ☒ Test values indicating whether an effect is present<br>*Provide confidence intervals or give results of significance tests (e.g. P values) as exact values whenever appropriate and with effect sizes noted.* |
| ☐ | ☒ A clear description of statistics including central tendency (e.g. median, mean) and variation (e.g. standard deviation, interquartile range) |
| ☐ | ☒ Clearly defined error bars in all relevant figure captions (with explicit mention of central tendency and variation) |

*See the web collection on statistics for biologists for further resources and guidance.*

## Software

Policy information about availability of computer code

7. Software

Describe the software used to analyze the data in this study.

Standard PRISM software was used for data analysis

For manuscripts utilizing custom algorithms or software that are central to the paper but not yet described in the published literature, software must be made available to editors and reviewers upon request. We strongly encourage code deposition in a community repository (e.g. GitHub). *Nature Methods* guidance for providing algorithms and software for publication provides further information on this topic.

## Materials and reagents

Policy information about availability of materials

8. Materials availability

Indicate whether there are restrictions on availability of unique materials or if these materials are only available for distribution by a third party.

-Blood samples are available upon request through an MTA
-HIV p24 ELISA kits are available from a third party (Frederick National Laboratory for Cancer Research)
-All other materials are commercially available

9. Antibodies

Describe the antibodies used and how they were validated for use in the system under study (i.e. assay and species).

Antibodies used for this study are listed below. All of these antibodies are commercially available and validated for flow cytometry applications. Diltuions used for each assay are found on the vendor's website.
-Anti-human CD3 APC/Cy7 (Biolegend, clone HIT3a, Cat#300318)
-Anti-human CD3 BUV395 (BD Biosciences, clone HIT3a, Cat#740283)
-Anti-human CD3 AF700 (Biolegend, clone HIT3a, Cat#300324)
-Anti-human CD14 APC/Cy7 (Biolegend, clone M5E2, Cat#301820)
-Anti-human CD4 APC (Biolegend, clone OKT4, Cat#317416)
-Anti-HIV Gag p24 RD-1 (Beckman Coulter, HIV-1 core antigen, clone KC-57, Cat#6604667)
-Anti-human SERPINB9/PI-9 AF488 (BioRad, clone 7D8, Cat#MCA2540A488)
-Anti-human CD62L PE/Cy5 (Biolegend, clone DREG-56, Cat#304808)
-Anti-human CD8 AF700 (Biolegend, clone SK7, Cat#344724)
-Anti-human CD8 FITC (Biolegend, clone SK7, Cat#344704)
-Anti-human CD45RA BV605 (Biolegend, clone HI100, Cat#304134)
-Anti-human CD45RA BV650 (Biolegend, clone HI100, Cat#304136)
-Anti-human perforin PE/Cy7 (Biolegend, clone B-D48, Cat#353316)
-Anti-human granzyme A PerCp/Cy5.5 (Biolegend, clone CB9, Cat#507216)
-Anti-human granzyme B Pacific Blue (Biolegend, clone GB11, Cat#515408)
-Anti-human granzyme H biotinylated antibody (R&D, polyclonal, Cat#BAF1377)
-Anti-human granzyme K PE (Biolegend, clone GM26E7, Cat#370512)
-Anti-human granzyme M eFluor660 (ThermoFischer Scientific, clone 4B2G4, Cat#50-9774-42)
-Anti-human CD107a AF488 (Biolegend, clone H4A3, Cat#328612)
-Anti-human IFN-gamma BV510 (Biolegend, clone 4S.B3, Cat#502544)
-Anti-human MHC-I BV510 (Biolegend, clone W6/32, Cat#311436)
-Streptavidin BV510 (Biolegend, Cat#405234)
-Streptavidin BV650 (Biolegend, Cat#405232)

Other staining reagents used for flow cytometry studies are described below. All are commercially available and commercially validated.
-LIVE/DEAD Fixable Blue Dead Cell Stain Kit (ThermoFischer Scientific, Cat#L34962)
-LIVE/DEAD Fixable Near-IR Dead Cell Stain Kit (ThermoFischer Scientific, Cat#L34976)
-CellTrace Violet Cell Proliferation Kit (ThermoFischer Scientific, Cat#C34557)
-CellTrace FarRed Cell Proliferation Kit (ThermoFischer Scientific, Cat#C34564)
-Vybrant FAM Caspase-3 and -7 Assay Kit (ThermoFischer Scientific, Cat#V35118)
-CellROX Green Reagent (ThermoFischer Scientific, Cat#C10444)
-Phalloidin AF555 ((ThermoFischer Scientific, Cat#A34055)

Anti-CD3 and Anti-CD28 antibodies were used for activation of CD4+ T cells. Assays were optimized for maximal stimulation, with use of plate-bound anti-human CD3 (Biolegend, Cat#317315) at 2ug/mL and soluble anti-human CD28 (Biolegend, Cat#302923) at 2ug/mL.

10. Eukaryotic cell lines

a. State the source of each eukaryotic cell line used.

HEK293T17 cells were obtained from ATCC (Catalogue number CRL-11268)

b. Describe the method of cell line authentication used.

Cell lines were authenticated by ATCC

c. Report whether the cell lines were tested for mycoplasma contamination.

Cell lines were not tested for mycoplasma

d. If any of the cell lines used are listed in the database of commonly misidentified cell lines maintained by ICLAC, provide a scientific rationale for their use.

The original cell line was obtained from ATCC. This specific clone of this cell line is optimal for retrovirus production and was only used to produce infectious HIV.

## Animals and human research participants

Policy information about studies involving animals; when reporting animal research, follow the ARRIVE guidelines

11. Description of research animals

Provide all relevant details on animals and/or animal-derived materials used in the study.

No animals were used for this study

Policy information about studies involving human research participants

12. Description of human research participants

Describe the covariate-relevant population characteristics of the human research participants.

This study involved the use of blood samples from antiretroviral treatment naive HIV+ patients who controlled plasma virus RNA levels to less than 2000 RNA copies/mL. Blood samples from healthy donors were also included in the study.

nature research

Corresponding author(s): Bruce D. Walker

# Flow Cytometry Reporting Summary

Form fields will expand as needed. Please do not leave fields blank.

## Data presentation

For all flow cytometry data, confirm that:

☒ 1. The axis labels state the marker and fluorochrome used (e.g. CD4-FITC).

☒ 2. The axis scales are clearly visible. Include numbers along axes only for bottom left plot of group (a 'group' is an analysis of identical markers).

☒ 3. All plots are contour plots with outliers or pseudocolor plots.

☒ 4. A numerical value for number of cells or percentage (with statistics) is provided.

## Methodological details

| | |
|---|---|
| 5. Describe the sample preparation. | Isolated cell populations from human PBMCs were treated as described in the Methods section (overnight resting or co-cultures), followed by harvesting and staining with the indicated panels of antibodies and a LIVE/DEAD stain (all commercially available). Cells were fixed, and where indicated, permeabilized for intracellular staining. All samples were analyzed by flow cytometry or imaging flow cytometry within 24 hours of staining. |
| 6. Identify the instrument used for data collection. | FACSCanto LSR Fortessa instrument (BD Biosciences) was used to acquire flow cytometry samples, while the Amnis ImageStream X Mark II (EMD Millipore) was used to acquire imaging flow cytometry samples. |
| 7. Describe the software used to collect and analyze the flow cytometry data. | FACSDiva software (BD Biosciences) was used to acquire the flow cytometry data while FlowJo, version 9.8.1, (Tree Star) was used to analyze these data. IDEAs Software 6.0 (EMD Millipore) was used to acquire and analyze the imaging flow cytometry data. |
| 8. Describe the abundance of the relevant cell populations within post-sort fractions. | No sorting was used for this study |
| 9. Describe the gating strategy used. | Figure #1 (Elimination Assays):<br>-A gating strategy is provided in Supplemental Figure #2, showing the initial cell population gating (FSC-A versus SSC-A), the population from which was then gated on singlets (FSC-A versus FSC-H), the population from which was then gated on a CellTrace Violet negative population (CD3 or CD14 versus CellTrace Violet) to gate out the CellTrace Violet-stained effectors. Note, some of the macrophage samples yielded a CD14 and CellTrace Violet double positive population, which represents a macrophage population with phagocytosed CellTrace Violet effectors. This population was included in the target cell gate, while CD14 negative CellTrace Violet+ cells were excluded. In some cases, the macrophages would lose their CD14 expression and thus a CD14-low population was included in the target cell gate. The target populations were then gated on LIVE/DEAD negative population (CD3 or CD14+ and CD14-low versus LIVE/DEAD), the population from which was then assessed on a CD4 versus HIV Gag p24 plot. The uninfected (Mock) sample was used as a negative control to draw a gate for the infected cell population. Alternatively, for target cells loaded with peptide and stained with CellTrace FarRed, the LIVE/DEAD negative population was then assessed on a SSC-A versus CellTrace FarRed plot, in which the positive and negative populations were clearly distinguished. The final plots for infected cell populations or peptide-loaded CellTrace FarRed positive populations are shown in Figures 1a and d.<br><br>Figure #2 (Assessment of Casapse-3 activity and production of ROS species):<br>-For assessment of Caspase-3 activity staining, the infected cell population (as |

described in Figure 1), was analyzed on a Caspase-3 activity (Vybrant FAM Caspase-3 and -7 substrate) versus CD3 or CD14 plot. Fluorescence minus one (minus the caspase reagent) was used as a negative staining control to draw the Caspase-3 activity positive gate for CD4+ T cells and macrophages. A similar gating strategy was used for assessment of ROS species using the CellROX reagent. Fluorescence minus one (minus the CellRox reagent) was used as a negative staining control to draw the CellRox positive gate for CD4+ T cells and macrophages.

Figure #3 (Assessment of SERPIN B9 expression):
-For assessment of SERPINB9 staining, cells were initially gated on an FSC-A versus SSC-A plot, the population from which was then gated on singlets (FSC-A versus FSC-H), the population from which was then gated on LIVE/DEAD negative population (CD3 or CD14 versus LIVE/DEAD), the population from which was then assessed on a SERPINB9 versus HIV Gag p24 plot. The uninfected (Mock) sample was used as a negative control to draw a quadrant gate for the infected cell population, while the infected cell sample not stained with SERPINB9 (SERPINB9 fluorescence minus one) was used to draw a quadrant gate for the SERPINB9 positive population.

Figure #4 (Assessment of tetramer and perforin/granzyme expression)
-For assessment of tetramer staining, cells were initially gated on an FSC-A versus SSC-A plot, the population from which was then gated on singlets (FSC-A versus FSC-H), the population from which was then gated on the LIVE/DEAD negative population (CD3 versus LIVE/DEAD), the population from which was then gated on CD8+ T cells (CD3 versus CD8), the population from which was then assessed on a plot of CD3 versus CMV or HIV tetramer. Cells not stained with tetramer (tetramer fluorescence minus one) were used to draw the gate to distinguish tetramer positive populations (shown in Supplemental Figure 5a). Representative plots of tetramer staining are shown in Figures 4a and Supplemental Figure 5c.
-The CD8+ T cell population was also subjected to analysis on a CD62L versus CD45RA plot to gate the naive population (CD62L+CD45RA+). This naive population was used to draw the perforin and granzyme A, B, H, K and M quadrant gates as naive cells do not express these proteins (internal negative staining control). This gating strategy is shown in Supplemental Figure 5b. Representative flow plots are shown in Figure 4b.
-For experiments assessing perforin/granzyme expression on CD107a positive cells, live, CD8+ T cells were gated as described above, followed by analysis on a CD3 versus CD107a plot. CD8+ T cells that were not stimulated with target cells were used as a negative control to draw the CD107a positive gate. CD107a positive populations were then assessed on perforin versus granzyme A, B, H, K or M plots. CD8+ T cells not stained with perforin, granzyme A, B, H, K or M antibodies (fluorescence minus one staining controls) were used to draw the perforin versus granzyme quadrant gates (Shown in Supplemental Figure 5d). Representative plots for perforin versus granzyme A, B, H , K, and M staining for ex vivo and expanded CD8+ T cells are shown in Figure 4d.

Figure #5 (Assessment of MHC-I surface density using ImageStream and IDEAs Software)
-To assess the MHC-I surface density, focused CD4+ T cell and macrophage events were acquired using a histogram of Gradient RMS on Channel 1 (Brightfield), with all events above 50 gated. This population was then assessed on a dot plot of Channel 3 (Phalloidin AlexaFluor 555) area versus aspect ratio. Cells with an aspect ratio of 0.9-1.0, representing cells with near circular morphology, were gated. This population was then analyzed on a dot plot of LIVE/DEAD Near IR (Channel 12) intensity versus MHC-I-BV510 (Channel 8) Intensity. LIVE/DEAD negative cells were gated and analyzed on a subsequent dot plot of MHC-I-BV510 (Channel 8) intensity versus cell height (diameter in um). "Corrected" mean fluorescence intensity (MFI) and surface area of MHC-I-BV510 were calculated as described in the Methods. Representative plots of this gating strategy are shown in Supplemental Figure 6b.

Figure #5 (Assessment of CD107a and IFN-gamma expression)
-For assessment of CD107a and IFN-gamma staining, cells were initially gated on an FSC-A versus SSC-A plot, the population from which was then gated on singlets (FSC-A versus FSC-H), the population from which was then gated on the LIVE/DEAD negative population (CD3 versus LIVE/DEAD), the population from which was then

gated on CD8+ T cells (CD3 versus CD8), the population from which was then assessed on a plot of CD3 versus CD107a and a plot of CD3 versus IFN-gamma. CD8 + T cell samples that were stimulated with an uninfected target (mock stimulated) were used as negative controls to draw both the CD107a positive gate and the IFN-gamma positive gate. Representative plots of CD107a versus CD3 are shown in Figure 5b for both ex vivo CD8+ T cell and expanded CD8+ T cell samples.
-For assessment of IFN-gamma staining within the CD107a positive population, the IFN-gamma positive gate (described above) was applied to the CD107a positive population. Representative plots of IFN-gamma versus CD3 are shown in Figure 5d.

Figure 6 (Assessment of immunological synapses via ImageStream and IDEAs software)
-To assess immunological synapse formation between CellTrace Violet-stained effectors and CellTrace FarRed-stained, peptide-loaded targets, focused cell events were acquired using a histogram of Gradient RMS on Channel 1 (Brightfield), with all events above 50 gated. This population was then assessed on a dot plot of Channel 1 (Brightfield) area versus aspect ratio, with all cells gated (debris was excluded based on area). This population was then assessed on a dot plot of Channel 7 (CellTrace Violet) intensity versus Channel 11 (CellTrace FarRed) intensity. One gate was drawn to include all CellTrace FarRed positive events while another gate was drawn to include all CellTrace Violet and CellTrace FarRed double positive events. Representative plots of this gating strategy are shown in Figure 6a. Analysis of these gated populations is described in the Methods section.

Tick this box to confirm that a figure exemplifying the gating strategy is provided in the Supplementary Information. ☒